COOPERATIVE CONTROL OF HETEROGENEOUS SYSTEMS BASED ON IMMERSION AND INVARIANCE ADAPTIVE CONTROL

BY

IMIL HAMDA IMRAN

A Thesis Presented to the
DEANSHIP OF GRADUATE STUDIES

KING FAHD UNIVERSITY OF PETROLEUM & MINERALS

DHAHRAN, SAUDI ARABIA

In Partial Fulfillment of the
Requirements for the Degree of

MASTER OF SCIENCE

In

SYSTEMS AND CONTROL ENGINEERING

MAY 2015

KING FAHD UNIVERSITY OF PETROLEUM & MINERALS

DHAHRAN- 31261, SAUDI ARABIA

DEANSHIP OF GRADUATE STUDIES

This thesis, written by **IMIL HAMDA IMRAN** under the direction his thesis advisor and approved by his thesis committee, has been presented and accepted by the Dean of Graduate Studies, in partial fulfillment of the requirements for the degree of **MASTER OF SCIENCE IN SYSTEMS ENGINEERING.**

Dr. Sami El Ferik
(Advisor)

Dr. Adel F. Ahmed
Department Chairman

Dr. Samir Al-Amer
(Member)

M-Faizan

Dr. Muhammad F. Mysorewala
(Member)

Dr. Salam A. Zummo
Dean of Graduate Studies

عمادة الدراسات العليا
DEANSHIP OF GRADUATE STUDIES

28/6/15

Date

-

Dedicated to

Papa Rahimahullah, Mama, Uni, Irsal, and Ad

ACKNOWLEDGMENTS

First and foremost, I would like to express my highest gratitude to Almighty ALLAH, the most merciful the most gracious, for this achievement. I thank him for giving me life, knowledge and making my MS program a success.

I thank my advisor Dr. Sami El Ferik for his continuous guidance and direction in this research work. This thesis would not have been possible without it. I express my appreciation to Dr. Samir Al-Amer and Dr. Muhammad Faizan Mysorewala to be a part of my evaluation committee and for their fruitful suggestions.

I would also like to thank all my KFUPM graduate colleagues and friends who helped me in one way or the other. I thank Mr. Bagus, Mr. Omar and Mr. Siddig for helping me whenever I needed anything from them. Thanks to my friends Mr. Rio, Mr. Fahim, Mr. Mirza and Mr. Tausiff for their love and affection.

My hearty gratitude goes to my father, Ali Imran Danin *Rahimahullah* and my mother, Ilfayeti, for their innumerable sacrifices, struggles, vast patience abundant love, care and prayer throughout my life to make me reach this stage of qualification and success. I express my appreciation to my beloved sister and brothers, Uni, Irsal and Ad, for their support and encouragements.

TABLE OF CONTENTS

LIST OF TABLES

LIST OF FIGURES

LIST OF ABBREVIATIONS

2D	: Two Dimensions
3D	: Three Dimensions
DOF	: Degree of Freedom
NN	: Neural Network
I&I	: Immersion and Invariance
PD	: Proportional Derivative
UAV	: Unmanned Aerial Vehicle

ABSTRACT

Full Name : Imil Hamda Imran

Thesis Title : Cooperative Control of Heterogeneous Systems Based on Immersion and Invariance Adaptive Control

Major Field : Systems Engineering

Date of Degree : May, 2015

This thesis deals with adaptive cooperative control of heterogeneous systems moving together in a given formation. In this study, we consider the formation of nonholonomic mobile robots and quadrotor UAV. The controller is designed based on the I&I adaptive approach. I&I adaptive is a framework for adaptive stabilization of nonlinear systems with uncertain parameters.

We investigate the tracking control of heterogeneous system robots with uncertainties in the dynamics. I&I adaptive control regulates the position of both the nonholonomic mobile robot and quadrotor UAV. The results demonstrate that the I&I adaptive cooperative control to track the desired path in particular formation. We compare performance of I&I adaptive with L1 adaptive controller. The simulation results show that the I&I adaptive is better to generate the heterogeneous robots to follow the desired formation.

We also develop cooperative control of nonholonomic mobile robots based on neuro I&I adaptive, where Neural Network (NN) generates the nonlinearity of dynamics and I&I computes the adaptation weight of NN. We compare the effectiveness of neuro I&I with I&I and L1 adaptive controllers. In simulation, all of the control strategies are able to follow the desired formation.

ملخص الرسالة

الاسم الكامل: عمل حمدا عمران

عنوان الرسالة: التحكم التعاوني للانظمه الغير متجانسه على اساس طريقه التحكم المتكيفه اي & اي

التخصص: هندسه النظم

تاريخ الدرجة العلمية: مايو 2015

تتناول هذه الاطروحه التحكم التعاوني المتكيف للانظمه غير المتجانسه التي تتحرك مع بعض في تشكيل معين. في هذه الدراسه، ندرس تشكيل الروبوتات المتنقله متغيره العوامل على طول المسار و الطائره بدون طيار. نظام المتحكم يصمم على اساس طريقه I&I المتكيفه. بنيه طريقه I&I يمكنها من التكيف لضمان استقرار الانظمه غير الخطيه مع قيم غير مؤكده للعوامل.

قمنا بدراسة تتبع التحكم للانظمه الآليه الغير المتجانسه مع قيم غير مؤكده للعوامل للبنيه المتحركه. المتحكم المتكيف I&I يضبط مكان كل من الروبوتات المتنقله متغير العوامل على طول المسار و الطائره بدون طيار. النتائج تظهر ان طريقه I&I للتحكم التعاوني المتكيف استخدمت لتتبع المسار المرغوب لتشكيل معين. نحن قمنا بمقارنه اداء طريقه I&I مع طريقه L1 المتكيفه. أظهرت النتائج ان طريقه I&I المتكيفه افضل في انتاج تشكيل مطلوب للروبوتات المتنقله متغير العوامل.

كذلك نحن طورنا تحكم تعاوني للروبوتات المتنقله متغيره العوامل باستخدام I&I العصبيه، حيث ان الشبكه العصبيه تنتج العوامل الغير خطيه للبنيه المتحركه و طريقه I&I تحسب الثقل المتكيف للشبكه العصبيه. ثم قمنا بمقارنه اداء المتحكمات لكل من I&I العصبيه مع I&I و L1 المتكيفه. بأستخدام المحاكاه، وجدنا ان كل طرق التحكم لها القدره على تتبع التشكيل المطلوب.

CHAPTER 1

INTRODUCTION

1.1 Motivation

Autonomous mobile robots and quadrotor Unmanned Aerial Vehicle (UAV) have acquired the attention of many researchers all around the world. We can find the mobile robots and quadrotors being employed in home, industry, military, entertainment, and security applications. The mobile robot is integrated with camera, sensor, actuator, and weaponry to achieve the desired target.

The research present here is mainly focused on nonholonomic type of mobile robots. The researchers from various research institutions and companies are working on the development of nonholonomic mobile robots in order to increase its accuracy, precision, repeatability and overcome its limitations. In the field of control of nonholonomic mobile robots, many researchers are working on problems related to trajectory tracking control pertaining to its position and velocity. They proposed many control strategies in order to make these devices more advanced, automatic, and intelligent. Also, there is intensive research dedicated to improve the existing control strategies. The initial literature review of nonholonomic mobile robot control is discussed in section 1.2.1.

Quadrotor UAVs are special type of aerial vehicle without any direct contact with human operating both autonomously and remotely. These UAVs are used in applications to minimalize the risk of human life such as working in hazardous environment, military surveillances and deep sea explorations. Quadrotor UAV is integrated with sensors, actuators, cameras and various other equipment depending on the type of applications. For example, in military surveillance purpose UAV is integrated with sensors and cameras, which help to track the target and make them to take appropriate action.

Many researchers are investigating different control strategies in order to control quadrotor UAV more efficiently. They have worked with regard to overcome the control limitations, thus solve the control issue and making the quadrotor UAV operates more autonomously and smoothly. A brief literature review on quadrotor UAV control can be seen in section 1.2.2.

Formation control techniques, which are used to control multi-robots, have attracted many researchers in recent years. The advantage of this control technique is that one can design independent controllers for every agent of the multi-agent system. The estimation of robot parameters such as position and velocity play an important part in designing any controller.

In this thesis, the design of adaptive cooperative control for nonholonomic mobile robot and quadrotor UAV based on I&I is proposed. The nonholonomic mobile robot and quadrotor UAV are commanded to follow a certain path while maintaining a particular formation. Thus, the multi-robot will move together and keep the desired formation with each other based on potential fields-based control. In potential field control, the center potential attracts each agent to the center while the inter-agent potential repulses two neighboring agents to avoid collision. We compare the effectiveness of I&I with L1 adaptive controllers for formation control of heterogeneous systems.

We also propose a neural-network-based I&I adaptive controller for formation control of nonholonomic mobile robots. Neuro-I&I adaptive is a framework for adaptive stabilization of nonlinear systems with uncertain parameters. Neural Network (NN) generates the nonlinearity of dynamics and I&I computes the adaptation weight of NN. Then we compare the effectiveness of neuro I&I with I&I and L1 adaptive controllers.

1.2 Literature Review

1.2.1 Feedback Control of Nonholonomic Mobile Robot

Research on mobile robot has seen a rapid increase in recent times. Researchers previously have worked to control the trajectory tracking of mobile robots which is one of the main issues in the real applications. Both the kinematic mobile robot and dynamic controller have to be considered in designing an appropriate controller. Adaptive control and Lyapunov stability theory are techniques used to control the nonholonomic mobile robot [3].

Two-wheeled mobile robot tracking control having more inputs than outputs was discussed in [4]. The inverse of the decoupling matrix in the input-output linearization did not exist when the number of inputs is not equal to the outputs. Hence, a modified input-output linearization technique is designed, a generalized inverse is used to solve it.

NN controllers possess a fast learning convergence and simple algorithm for tracking the trajectory of mobile robot was developed in [5]. The integration of a kinematic control and a torque control using a NN for nonholonomic mobile robot was developed in [9]. They proposed backstepping for kinematic control and Lyapunov theory to guarantee the stability. Their algorithm applied for tracking the trajectory, path following and stabilization.

Cascaded controllers proposed in [6] to track the trajectory of nonholonomic mobile robot. The tracking controller uses two cascades in this case. The first fuzzy controller produces a variable presenting the path curvature and one input of the second fuzzy controller. Adaptive Neuro Fuzzy Inference System (ANFIS) is proposed as the second stage controller to track the desired path of mobile robots.

Adaptive control to track the desired trajectory of a wheeled nonholonomic mobile robot (WMR) with unknown dynamics and parameters applied in [7]. They design the robust backstepping based on NNs without considering the previous knowledge of the dynamics. The gains of kinematic controller designed to enhance tracking characteristics and minimize the velocity error.

An adaptive tracking controller approach with output feedback is designed in [8] to minimize that the tracking errors of a nonholonomic mobile robot. They proposed a new adaptive control scheme to determine the linear and angular velocities respectively to overcome system parameters which are not known and also a quadratic term of immeasurable states in the mobile robot dynamic system and couplings. Adaptive tracking controller was developed in [2] using the adaptive backstepping approach for the integration of kinematic and torque controller with unknown parameters exists for a nonholonomic mobile robot. A sliding-mode control was proposed in [11] for mobile robots in two-dimensional polar coordinates. The integration of kinematic control and tracking trajectory is applied in [12] based on adaptive fuzzy for nonholonomic mobile robot. Neuron-based adaptive controller presented in [13] for trajectory tracking of nonholonomic mobile robot without velocity measurement.

A controller using nonlinear PID-based analog NNs was developed in [14] to follow the desired path of nonholonomic mobile robot and cover nonlinearity uncertainties and disturbance issues. An adaptive robust tracking controller using modified feedback linearization proposed in [17] for trajectory tracking for mobile robots with parametric and nonparametric uncertainties.

Backstepping-like feedback linearization applied a cascaded kinematic and dynamic linearization of wheeled mobile robots for tracking control in [15]. Two controllers using backstepping based on kinematic model was designed in [16] separately for tracking control of nonholonomic mobile robot. Lyapunov theory applied to guarantee the stability and adaptive robust method proposed in [18] for trajectory tracking control of electrically driven wheeled mobile robots with uncertainties parameter.

1.2.2 Feedback Control of Quadrotor UAV

The output feedback controller was designed in [19] via Lyapunov theory analysis for tracking control of nonlinear small-scale UAVs quadrotor which only position and angles are measurable. Sliding mode control based on feedback linearization compared with sliding mode based on backstepping for tracking control presented in [20] which chatting phenomenon occurred in sliding mode control and complex Lyapunov function was not required according to backstepping method. Feedback linearization controller and adaptive sliding mode controller were proposed in [22] for nonlinear quadrotor helicopter. The sliding mode controller is able to control the system under noisy condition and estimate uncertainty effectively. In [26] backstepping was implemented for UAVs to track the trajectory consisting of translational dynamics and attitude kinematics. The experiment in real indoor quadrotor that showed the result verifies the validity proposed theory.

NN based output feedback controller applied in [21] a quadrotor UAV with uncertain nonlinear terms like aerodynamic friction and blade flapping. NNs and output feedback were developed in [23] to control the nonlinear quadrotor UAV. They applied NNs to learn the complete dynamic of UAV online including uncertain nonlinear part. NN virtual control allowed four control inputs to control 6 DOF. The output feedback control scheme is applied to control the presence of unknown nonlinear dynamics and disturbances of UAV.

Time varying adaptive controller proposed in [24] for an underactuated quadrotor UAV with uncertainties associated with mass, inertia matrix, and aerodynamic damping coefficients. They used Lyapunov theory to track the error of position and yaw rotation. Direct and indirect Model Reference Adaptive Control (MRAC) was developed in [25] to track the desired trajectory of low cost quadrotor UAV. The adaptive controller is able to increase the robustness to uncertainties parameter and mitigate the effects of a loss-of-thrust anomaly effectively.

1.2.3 Cooperative Control

Feedback linearization to control multiple robot moving together was developed in [27] around an obstacle in a formation based on the leader - follower approach. The information of local sensor is used to stabilize the distance and orientation of followers. They showed that controller is able to control arbitrarily large numbers of robots which move together in general type formation.

A framework was developed [28] for trajectory control of the multiple nonholonomic mobile robots moving together with range sensors. Lyapunov theory applied to find the stability condition of closed-loop hybrid system. Their framework allowed the system switch automatically between continuous-state control laws to achieve a desired trajectory. The synthesis of controllers was addressed in [30] for large groups of robots and sensors. They proposed controllers allowed robots to centralize curve S as trajectory with consider weighted sums of radial basis functions which give a high degree of control.

A framework was developed in [29] for cooperative control of robots. The controller and planner derived based on potential field that give benefit for complex group inter-action. They showed the cooperative control based on potential filed successfully in many cases without showing the sensitivity to parameters. The framework to control multiple nonholonomic mobile robots moving together in leader-follower formation was developed in [32]. They applied backstepping to accommodate the dynamics of the robot the formation in contrast with kinematic-based formation controllers. Lyapunov theory was used to guarantee the stability of nonholonomic mobile robots.

Decentralized controllers were developed in [31] for a group robot to follow the desired two-dimensional (2D) geometric pattern. The information on range sensors was used to allow robot to keep the distance from each other. Decentralized controller to control the formation mobile robot was developed in [33]. The artificial potential fields were used to obtain the formations. Lyapunov theory applied to find the asymptotic stability of the system. Experiment result successfully verified to validate the theory.

1.3 Problem Formulation and Objective

Based on the initial literature review, we consider the objective of this thesis as mentioned below

1. To develop potential field based formation for heterogeneous systems, in this study we consider the formation of nonholonomic mobile robot and quadrotor UAV.
2. To design adaptive cooperative control based on I&I method for the above heterogeneous systems and compare it with L1 adaptive cooperative control.

1.4 Thesis Organization

In order to achieve the objective mentioned in the previous section, we design the structure of the thesis as following

- Chapter 1, Introduction. Contains motivation, literature review, problem formulation and objectives.
- Chapter 2, Preliminary. Contains dynamics of nonholonomic mobile robot, dynamics of quadrotor UAV, Nonlinear control approach: L1 adaptive control methodology, I&I adaptive control methodology.

- Chapter 3, Adaptive Control Design. Contains adaptive control of nonholonomic mobile robot and quadrotor UAV based on I&I and L1 in case of presence of parameter uncertainty on the dynamics, Cooperative control based on neuro I&I for nonholonomic mobile robots.
- Chapter 4, Cooperative Control Design. Contains design cooperative control for heterogeneous systems based on potential field.
- Chapter 5, Simulation Results. The simulation conducts to validate the I&I and L1 adaptive control performance for cooperative control of heterogeneous systems.
- Chapter 6, Conclusion. Concludes all the work in the thesis and suggestion for possible extension in future work.

CHAPTER 2

PRELIMINARY

2.1 Introduction

This chapter presents the modeling of nonholonomic mobile robots and quadrotor UAV. Firstly, we introduce basic concepts of nonholonomic mobile robots and quadrotor UAV, followed by physical parameter used in that dynamical systems. We also study the basic idea about I&I and L1 adaptive control methodology.

2.2 Dynamics of nonholonomic mobile robot

In this study, we use nonholonomic mobile robot, which is defined in [1][2][40]. The mobile robot which have 2-dimensional coordination space system are subjected to constraints which are described in general coordinates as given by

$$M(q)\ddot{q} + V_m(q,\dot{q})\dot{q} + F(\dot{q}) + G(q) + \tau_d = B(q)\tau - A^T(q)\lambda \qquad (2.1)$$

where

$M(q)\epsilon\mathcal{R}^{nxn}$: Symmetric PD inertia matrix

$V_m(q,\dot{q})\epsilon\mathcal{R}^{nxn}$: Centripetal and corioles matrix

$F(\dot{q})\epsilon\mathcal{R}^{nx1}$: Surface friction

$G(q)\epsilon\mathcal{R}^{nx1}$: Gravitational vector

$\tau_d\epsilon\mathcal{R}^{nx1}$: Unknown disturbance

$B(q)\epsilon\mathcal{R}^{nxr}$: Input transformation matrix

$\tau\epsilon\mathcal{R}^{nx1}$: Input vector

$A^T(q)\epsilon\mathcal{R}^{mxn}$: matrix associated with constraints

$\lambda\epsilon\mathcal{R}^{mx1}$: Constraint forces vector

All kinematic equality constraints are considered not to be time-dependent

$$A(q)\dot{q} = 0 \tag{2.2}$$

$A(q)$ is a full rank matrix of a set of smooth and linearly independent vector fields in null space,

$$S^T(q)A^T(q) = 0 \tag{2.3}$$

Vector time function $v(t)\epsilon\mathcal{R}^{n-m}$ can be found by considering (2.2) and (2.3),

$$\dot{q} = S(q)v(t) \tag{2.4}$$

where

$$S(q) = \begin{bmatrix} \cos\theta & -d\sin\theta \\ \sin\theta & d\cos\theta \\ 0 & 1 \end{bmatrix} \tag{2.5}$$

$$v = \begin{bmatrix} v \\ \omega \end{bmatrix} = \begin{bmatrix} v_1 \\ v_2 \end{bmatrix} \tag{2.6}$$

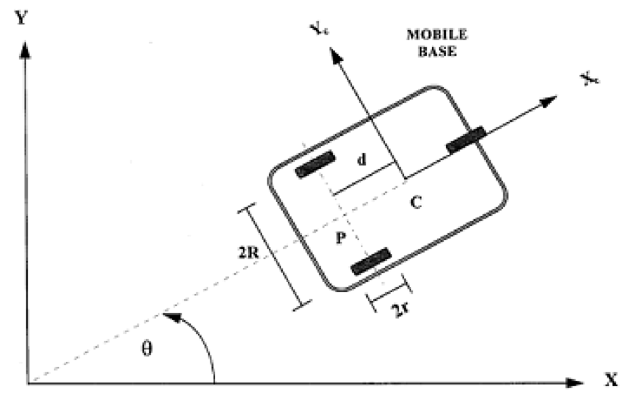

Figure 2.1 A nonholonomic car-like mobile robot. [1]

Figure 2.1 shows the position of nonholonomic mobile robot in an inertial Cartesian frame $\{O, X, Y\}$ which is presented by the vector $q = [x, y, \theta]^T$. $S(q)$ is the transformation matrix which transforms the velocities of the vehicle coordinates 'v' to Cartesian coordinates velocities $\dot{q}$.

Now the system (2.1) transforms and become appropriate for control consideration with differentiating (2.4) and substituting it into (2.1). The resulting equation is multiplied by S^T. The final equations of motion of the nonholonomic mobile robot will be given

$$S^T M S \dot{v} + S^T\left(M\dot{S} + V_m S\right)v + \bar{F} + \bar{\tau}_d = S^T B \tau \tag{2.7}$$

where $v(t)\epsilon\mathcal{R}^{n-m}$ is a vector of the velocity. Equation (2.7) can be written as

$$\bar{M}(q)\dot{v} + \bar{V}_m(q, \dot{q})v + \bar{F}(v) + \bar{\tau}_d = \bar{B}\tau \tag{2.8}$$

$$\bar{\tau} = \bar{B}\tau \tag{2.9}$$

where,

$\bar{M}(q)\epsilon\mathcal{R}^{nxn}$: Symmetric PD inertia matrix

$\bar{V}_m(q,\dot{q})\epsilon\mathcal{R}^{nxn}$: Centripetal and corioles matrix

$\bar{F}(\dot{q})\epsilon\mathcal{R}^{nx1}$: Surface friction

$\bar{\tau}_d$: Unknown disturbance

$\bar{\tau}\epsilon\mathcal{R}^{rx1}$: Input transformation matrix

The matrices defining the dynamics of nonholonomic mobile robot with mass m based on figure 1 are presented in (2.1) where,

$$M(q) = \begin{bmatrix} m & 0 & md\sin\theta \\ 0 & m & -md\cos\theta \\ md\sin\theta & -md\cos\theta & I \end{bmatrix} \tag{2.10}$$

$$\bar{V}_m(q,\dot{q}) = \begin{bmatrix} 0 & \frac{r^2}{2R}md\dot{\theta} \\ -\frac{r^2}{2R}md\dot{\theta} & 0 \end{bmatrix} \tag{2.11}$$

$$G(q) = 0 \tag{2.12}$$

$$B(q) = \frac{1}{r}\begin{bmatrix} \cos\theta & \cos\theta \\ \sin\theta & \sin\theta \\ R & -R \end{bmatrix} \tag{2.13}$$

$$\tau = \begin{bmatrix} \tau_1 \\ \tau_2 \end{bmatrix} \tag{2.14}$$

Table 2.1 shows the parameters of nonholonomic mobile robots used in this thesis.

Table 2.1. The vehicle parameters

Parameter	Value	Unit
m	10	kg
I_0	5	kgm^2
R	0.5	m
r	0.05	m
d	0.8	m

where

$$I = I_0 + \Delta I \tag{2.15}$$

where I_0 is the initial value of inertia and ΔI changes in the value of inertia when the robot moves.

2.3 Dynamics of Quadrotor UAV

In this study, we use Quadrotor UAV, which is defined in [38][39][41]. The motions of quadrotor UAV are related to the translational and rotational motions. In translational motions, quadrotor UAV is able to move forward/backward, lateral, and vertical. In rotational motions quadrotor UAV has roll, pitch, and yaw motions. The quadrotor UAV has four propellers as basic movements. The four possible basic movements of the quadrotor UAV includes throttle (u), roll (τ_p), pitch (τ_q), and yaw (τ_r).

The motion of Quadrotor UAV in 6-DOF consider two coordinate frames. The position and orientation are expressed with respect to the inertial frame and both linear and angular velocities are described with respect to the body frame. Figure 2.2 shows two coordinate frames of quadrotor UAV.

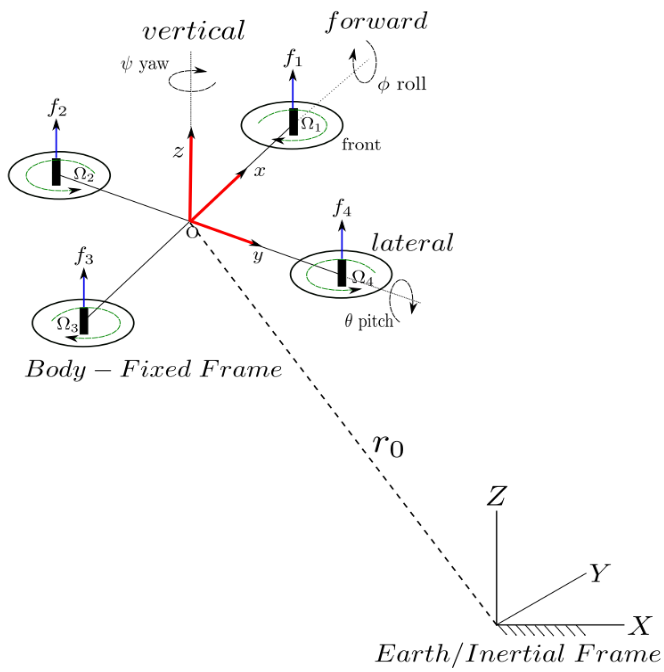

Figure 2.2 Body-fixed and earth reference frame. [41]

The 6 DOF motion of a quadrotor UAV is expressed as

$$\eta = [{\eta_1}^T, {\eta_2}^T]^T \qquad \eta_1 = [x, y, z]^T \qquad \eta_2 = [\phi, \theta, \psi]^T \tag{2.16}$$

$$\upsilon = [{\upsilon_1}^T, {\upsilon_2}^T]^T \qquad \upsilon_1 = [u, v, w]^T \qquad \upsilon_2 = [p, q, r]^T$$

where η is composed of the position vector. v is the velocity vector, υ_1 is linear velocity and υ_2 is angular velocity. The inertial frame and the body frame have the dynamic coupling which is given by a velocity transformation.

$$\dot{\eta_1} = J_1(\eta_2)\upsilon_1 \qquad \dot{\eta_1} = {J_1}^{-1}(\eta_2)\dot{\eta_1} \tag{2.17}$$

where the transformation matrix $J_i(\eta_2),\ i = 1{,}2$ are functions of the Euler angles. The transformation matrix which relate the translational velocity in the body frame to the inertial frame is given by

$$J_1(\eta_2) = \begin{bmatrix} cos\psi cos\theta & -cos\psi cos\phi + cos\psi sin\theta sin\phi & sin\psi sin\phi + cos\psi cos\theta sin\phi \\ sin\psi cos\theta & cos\psi cos\phi + cos\psi sin\theta sin\phi & -cos\psi sin\phi + sin\psi cos\phi sin\theta \\ -sin\theta & cos\theta sin\phi & cos\phi cos\theta \end{bmatrix} \tag{2.18}$$

Lagrangian for the generalized coordinate is presented by

$$L(q, \dot{q}) = T_{trans} + T_{tot} - U = \frac{1}{2} m\dot{\eta_1}^T \dot{\eta_1} + \frac{1}{2} m\dot{\eta_2}^T \dot{\eta_2} - mgz \tag{2.19}$$

where T_{trans} is the kinetic energy for the translational motion, T_{tot} is the kinetic energy of the orientation, U is potential energy and I_η is

$$I_\eta = \left({J_2}^{-1}\right)^T I_M {J_2}^{-1}, \qquad I_M = \begin{bmatrix} I_{xx} & 0 & 0 \\ 0 & I_{yy} & 0 \\ 0 & 0 & I_{zz} \end{bmatrix} \tag{2.20}$$

where τ is the torque responsible for the rotational motion. The drag terms are represented by notations k_r for the rotational drag, and k_t for the translational drag.

The translational dynamics of the quadrotor UAV is expressed as

$$\ddot{\eta}_1 = -gz_e + J_1(\eta_2)\frac{u}{m}z_e - \frac{k_t}{m}\dot{\eta}_1 \quad (2.21)$$

where τ is the torque for rotational movements, k_r is for the rotational drag, and k_t is for the translational drag, $z_e = [0, 0, 1]^T$and $u = f_1 + f_2 + f_3 + f_4$. f_i's are the upward lifting forces computed and are given by $f_i = k_i{\Omega_i}^2$. The rotational motion of the quadrotor UAV on the body frame is given by

$$\dot{v}_2 = I^{-1}(-(v_2 \times Iv_2) - I_R(v_2 - z_e)\Omega - k_r v_2 + \tau) \quad (2.22)$$

where I_M is the total inertia of the quadrotor UAV, I_R is the propeller inertia, $\times$ represents the vector cross product, k_r is the rotational drag coefficient, and $\Omega = \Omega_1 - \Omega_2 + \Omega_3 - \Omega_4$. The force and torques acting around the body is given by

$$\begin{bmatrix} \tau \\ u \end{bmatrix} = \begin{bmatrix} \tau_p \\ \tau_q \\ \tau_r \\ u \end{bmatrix} = \begin{bmatrix} 0 & l & 0 & -l \\ l & 0 & -l & 0 \\ d & -d & d & -d \\ 1 & 1 & 1 & 1 \end{bmatrix} \begin{bmatrix} f_1 \\ f_2 \\ f_3 \\ f_4 \end{bmatrix} \quad (2.23)$$

where l is the distance from the motor to the center of mass, and d is the ratio between drag and thrust coefficient of the blade. Table 2.2 shows the parameters of quadrotor UAV used in this thesis, these parameters are obtained in [10][41].

Table 2.2. The quadrotor UAV parameters

Mass	m	$0.52\ kg$
Gravity Acceleration	g	$9.8\ m/s^2$
Translational Drag Coefficient	k_t	0.95
Rotational Drag Coefficient	k_r	0.105
Ratio Between Drag and Thrust Coefficient	d	$7.5e^{-7}\ kgm^2$
Inertia Coefficient on x-axis	I_x	$0.0069\ kgm^2$
Inertia Coefficient on y-axis	I_y	$0.0069\ kgm^2$
Inertia Coefficient on z-axis	I_z	$0.0129\ kgm^2$
Arm Length	L	$0.205\ m$
Propoller Inertia	R	$3.36e^{-5}kgm^2$

2.4 Nonlinear Control Theory

2.4.1 Immersion and Invariance Adaptive Control

Research related to I&I have been developed in recent years, I&I control developed for underactuated cart-pendulum system [34], for quadrotor UAV [41], antagonistic joint with nonlinear mechanical stiffness [35] and stabilization of a synchronous generator with a controllable series capacitor [36]. The I&I adaptive control of nonlinear systems introduce in [37].

Let's consider the system structure

$$\dot{x} = f(x) + Gu \tag{2.24}$$

where $x \in \mathbb{R}^n$ is the state of the system and $u \in \mathbb{R}^m$ is the control of the system with an equilibrium point $x_* \in \mathbb{R}^n$ to be stabilized. We assume find rhe mapping with $p < n$

$$\alpha: \mathbb{R}^p \to \mathbb{R}^p \qquad \pi: \mathbb{R}^p \to \mathbb{R}^n \tag{2.25}$$

$$c: \mathbb{R}^p \to \mathbb{R}^m \qquad \phi: \mathbb{R}^n \to \mathbb{R}^{n-p}$$

$$\psi: \mathbb{R}^n \to \mathbb{R}^{n\times(n-p)}$$

such that the following manifold.

The target system

$$\dot{\xi} = \alpha(\xi) \tag{2.26}$$

where $\xi \in \mathbb{R}^p$ is the state with asymptotically stable equilibrium at $\xi_* \in \mathbb{R}^p$ and $x_* = \pi(\xi_*)$.

The immersion condition for all $\xi \in \mathbb{R}^p$ define in (2.27)

$$f\big(\pi(\xi)\big) + g\big(\pi(\xi)\big)c\big(\pi(\xi)\big) = \frac{\partial \pi}{\partial \xi}\alpha(\xi) \tag{2.27}$$

and the set identity of implicit manifold

$$\{x \in \mathbb{R}^n | \phi(x) = 0\} = \{x \in \mathbb{R}^n | x = \pi(\xi)\}\, for\ some\ \xi \in \mathbb{R}^p \tag{2.28}$$

holds

All trajectories of the system can be defined as

$$\dot{z} = \frac{\partial \phi}{\partial x}\big(f(x) + g(x)\psi(x,z)\big) \tag{2.29}$$

and

$$\dot{x} = f(x) + g(x)\psi(x,z) \tag{2.30}$$

are bounded and satisfy $\lim_{t\to\infty} z(t) = 0$.

Then x_* is an asymptotically equilibrium of the closed loop system

$$\dot{x} = f(x) + g(x)\psi\big(x,\psi(x)\big) \tag{2.31}$$

2.4.2 L1 Adaptive Control

L1 adaptive control method was developed in [42] with robustness and fast adaptation. This control strategy applied in various mechanical systems such as aeroplane needed very high accuracy. We describe the L1 adaptive control methodology in this part.

Consider the control structure of the systems

$$u(t) = u_m(t) + u_{ad}(t) \qquad u_m(t) = -{k_m}^T x(t) \tag{2.32}$$

where $u_{ad}(t)$ is adaptive control input and $k_m \in \mathbb{R}^n$ renders $A_m \triangleq A - b{k_m}^T$ Hurwitz. The state feedback k_m leads to the partial closed loop system

$$\dot{x}(t) = A_m x(t) + b\big(\theta^T x(t) + u_{ad}(t)\big) \tag{2.33}$$

$$x(0) = x_0 \qquad y(t) = c^T x(t)$$

We consider state predictor as linearly parameterized system

$$\dot{\hat{x}}(t) = A_m \hat{x}(t) + b\left(\hat{\theta}^T x(t) + u_{ad}(t)\right) \tag{2.34}$$

$$\hat{x}(0) = x_0 \qquad \hat{y}(t) = c^T \hat{x}(t)$$

where $\hat{x}(t) \in \mathbb{R}^n$ is state of the predictor and $\hat{\theta}(t) \in \mathbb{R}^n$ is estimation of θ.

Equation (2.35) express projection-type of adaptation law

$$\dot{\hat{\theta}}(t) = \Gamma Proj\left(\hat{\theta}(t), -\tilde{x}^T(t) P b x(t)\right), \qquad \hat{\theta}(0) = \hat{\theta}_0(t) \in \Theta \tag{2.35}$$

where the state predictor error is equal to $\tilde{x}(t) \triangleq \hat{x}(t) - x(t)$,$\Gamma \in \mathbb{R}^+$ is the gain of adaptation law rate, and $P = P^T > 0$ with $Q = Q^T > 0$ is the matrix solved Lyapunov equation ${A_m}^T P + P A_m = -Q$.

The projection is confined to the set Θ that can be found in [42].

The adaptive control input is defined in Laplace transform

$$u_{ad}(s) = -C(s)\left(\hat{\eta}(s) - k_g r(s)\right) \tag{2.36}$$

where $k_g \triangleq -\frac{1}{(c^T {A_m}^{-1} b)}$ and $C(s)$ is a BIBO-stable strictly proper transfer function with $C(0) = 1$. The initial of state-space realization is assumed zero.

CHAPTER 3

ADAPTIVE CONTROL DESIGN

3.1 Introduction

This chapter deals with adaptive control design for both nonholonomic mobile robot and quadrotor UAV. For nonholonomic mobile robot I&I, L1 and neuro I&I adaptive controllers are designed, and for quadrotor UAV I&I and L1 adaptive controllers are designed taking into account all the uncertain parameters and unknown dynamics of the system.

3.2 Nonholonomic Mobile Robot

Figure 3.1 shows control structure of nonholonomic mobile robot based on I&I and L1 adaptive. The robot moves to track the desired trajectory about in x as well as y direction. We apply cascaded controller where PD is the controller of outer loop and I&I and L1 adaptive is the controller of inner loop system. PD controller generates the linear and angular velocity of mobile robot using error position of nonholonomic mobile robot. The error position is the gap between the desired position of nonholonomic mobile robot x_d and y_d and the actual position x and y. The I&I and L1 adaptive compute the control input

τ of nonholonomic mobile robot. The actual linear and angular velocity of nonholonomic mobile robot are feedback input of inner loop system.

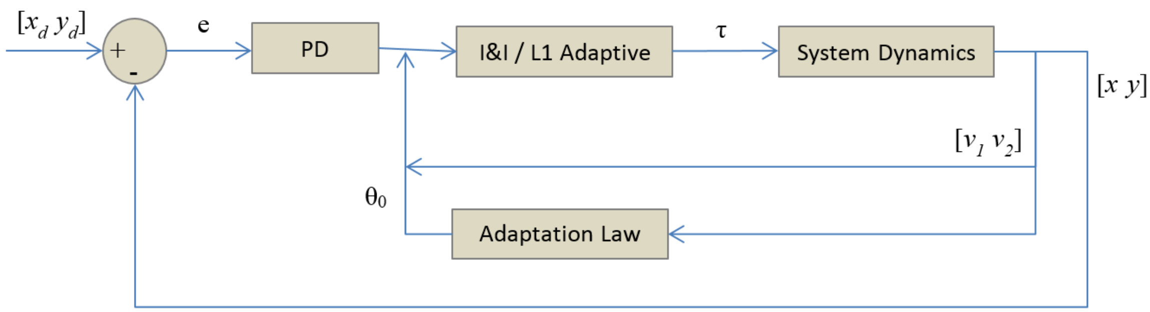

Figure 3.1 Control structure of single nonholonomic mobile robot based on I&I and L1 adaptive.

The robot moves to track the desired trajectory about in x as well as y direction. We apply tracking error position is to generate required input of NN. The error position is the gap between the desired position of nonholonomic mobile robot x_d and y_d and the actual position x and y. NN compute the nonlinearity of dynamics, and then I&I adaptive compute the weight of NN. The neuro I&I adaptive approach compute the control input τ of nonholonomic mobile robot.

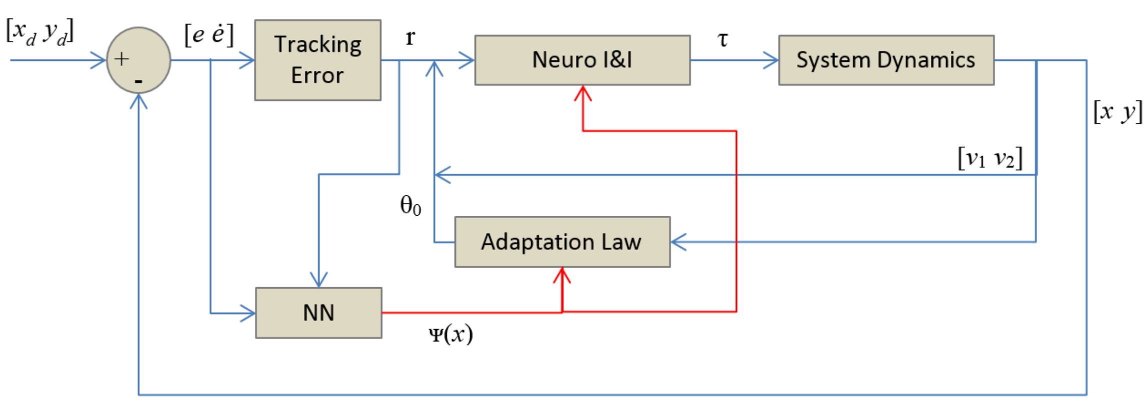

Figure 3.2 Control structure of single nonholonomic mobile robot based on neuro I&I adaptive.

3.2.1 Design of I&I Adaptive Control

The dynamic model of the given nonholonomic system can be written as:

$$\dot{v} = \bar{M}^{-1}(\bar{V}_m(q,\dot{q})v + \bar{F}(v) + \bar{\tau}_d + \bar{B}\tau) \tag{3.1}$$

$$\dot{v} = \bar{M}^{-1}(\bar{V}_m(q,\dot{q})v + \bar{F}(v) + \bar{\tau}_d + \bar{B}\tau) \tag{3.2}$$

$$\dot{v} = \bar{M}^{-1}\bar{V}_m(q,\dot{q})v + \bar{M}^{-1}\bar{F}(v) + \bar{M}^{-1}\bar{\tau}_d + \bar{M}^{-1}\bar{B}\tau \tag{3.3}$$

Equation (3.3) can also be expressed as

$$\dot{v} = f_0(v)\theta_0 + f_1(v) + \bar{M}^{-1}\bar{F}(v) + \bar{M}^{-1}\bar{\tau}_d + Gu \tag{3.4}$$

where

$$\tau \triangleq u \qquad G = \bar{M}^{-1}\bar{B} \qquad \theta_0 = \frac{1}{-md^2+I}$$

$$f_0(v) = \begin{bmatrix} 0 \\ \frac{dmr^2\dot{\theta}v_1}{2R} \end{bmatrix} \qquad f_1(v) = \begin{bmatrix} -\frac{dr^2\dot{\theta}v_2}{2R} \\ 0 \end{bmatrix}$$

Let us assume $\bar{F}(v) = 0$ and $\bar{\tau}_d = 0$. The controller design can be given by

$$u = G^{-1}(-f_0\theta_0 - f_1 - K_B v + K_F r) \tag{3.5}$$

where $K_F > 0$ is the feedforward gain, feedback gain $K_B > 0$ and r is the reference system.

In order to achieve the globally exponentially stable closed loop system we apply feedforward and feedback gains as

$$\dot{v} = -K_B v + K_F r \tag{3.6}$$

To apply I&I adaptive control on the dynamics, define the following implicit manifold as

$$z_0 = \hat{\theta}_0 - \theta_0 + \beta_0(v) \tag{3.7}$$

and the dynamic system is expressed by

$$\dot{z}_0 = \dot{\hat{\theta}}_0 + \frac{\partial \beta_0}{\partial v}\dot{v}$$

$$\dot{z}_0 = \dot{\hat{\theta}}_0 + \frac{\partial \beta_0}{\partial v}(f_0(v)\theta_0 + f_1(v) + Gu) \tag{3.8}$$

The adaptation law $\left(\omega\left(x, \hat{\theta}_l\right) = \dot{\hat{\theta}}_l\right)$ is selected as

$$\omega_0 = -\frac{\partial \beta_0(v)}{\partial v}\left(f_0(v)\left(\hat{\theta}_0 + \beta_0\right) + f_1(v) + Gu\right) \tag{3.10}$$

substituting these into (3.9) and (3.10), and utilizing (3.8) one will achieve

$$\dot{z}_0 = -\left(\frac{\partial \beta_0(v)}{\partial v} f_0(v)\right) z_0 \tag{3.11}$$

$\frac{\partial \beta_0(v)}{\partial v} = \gamma_0 {f_0}^T(v)$, where $\gamma_0 > 0$ is selected, the following is obtained

$$\lim_{n \to \infty} z(t) = 0 \qquad \Rightarrow \qquad \theta_l = \hat{\theta}_l + \beta\,(v) \tag{3.12}$$

The I&I adaptive control is expressed by

$$u = G^{-1}\left(-f_0\left(\hat{\theta}_0 + \beta_0\right) - f_1 - K_B v + K_F r\right) \tag{3.13}$$

3.2.2 Design of L1 Adaptive Control

The linearly parameterized of nonholonomic mobile robot dynamic in equation (3.4) can be rewritten as

$$\dot{x}(t) = A_m x(t) + b\left(f\big(t, x(t)\big) + \omega u_{ad}(t)\right) \tag{3.14}$$

$$x(0) = x_0 \qquad\qquad y(t) = c^T x(t)$$

where

$x \triangleq v_2,$ $\qquad A_m \in \mathbb{R}^{n\times n} \triangleq$ a known a desired Hurwitz matrix

$b = 1,$ $\qquad \omega = \theta_0,$ $\qquad u_{ad} \triangleq \tau \triangleq \mathcal{L}_1$adaptive control,

$$f\big(t, x(t)\big) \triangleq f_0(v)\theta_0 + f_1(v) + \bar{M}^{-1}\bar{F}(v) + \bar{M}^{-1}\bar{\tau}_d,\ c^T = I_{2\times 1} \tag{3.15}$$

Equation (3.4) can be rewritten as

$$\dot{x}(t) = A_m x(t) + b(\omega u_{ad} + \theta\|x\|_\infty + \sigma) \tag{3.16}$$

$$x(0) = x_0 \qquad\qquad y(t) = c^T x(t)$$

Let consider state predictor as linearly parameterized system in (3.16) as

$$\dot{\hat{x}}(t) = A_m \hat{x}(t) + b\big(\omega u_{ad} + \hat{\theta}\|x\|_\infty + \hat{\sigma}\big) \tag{3.17}$$

$$\hat{x}(0) = x_0 \qquad\qquad \hat{y}(t) = c^T \hat{x}(t)$$

where $\hat{x}(t) \in \mathbb{R}^n$ is state of the predictor, $\hat{y}(t) \in \mathbb{R}^n$ is predicted output and $\hat{\theta}$ and $\hat{\sigma}$ are estimation of θ and σ respectively.

We define the error dynamic of the system as

$$\dot{\tilde{x}}(t) = A_m\tilde{x}(t) + b\left(\omega u_{ad} + \tilde{\theta}\|x\|_\infty + \tilde{\sigma}\right), \qquad \tilde{x}(0) = x_0 \tag{3.18}$$

where the errors are equal to $\tilde{x}(t) \triangleq \hat{x}(t) - x(t)$, $\tilde{\theta}(t) \triangleq \hat{\theta}(t) - \theta(t)$ and $\tilde{\sigma}(t) \triangleq \hat{\sigma}(t) - \sigma(t)$.

We apply Lyapunov function to define the stability condition of the system

$$V\left(\tilde{x}, \tilde{\theta}, \tilde{\sigma}\right) = \tilde{x}^T P\tilde{x} + \frac{1}{\Gamma}\left(\tilde{\theta}^T\tilde{\theta} + \tilde{\sigma}^T\tilde{\sigma}\right) \tag{3.19}$$

Equation (3.20) is the derivative of Lyapunov candidate

$$\dot{V}\left(\tilde{x}, \tilde{\theta}, \tilde{\sigma}\right) = \dot{\tilde{x}}^T P\tilde{x} + \tilde{x}^T P\dot{\tilde{x}} + \frac{2}{\Gamma}\left(\tilde{\theta}^T\dot{\tilde{\theta}} + \tilde{\sigma}^T\dot{\tilde{\theta}}\right) \tag{3.20}$$

$$\dot{V}\left(\tilde{x}, \tilde{\theta}, \tilde{\sigma}\right) = -\tilde{x}^T P\tilde{x} + 2\tilde{x}^T Pb\left(\tilde{\theta}\|x\|_\infty + \tilde{\sigma}\right) + \frac{2}{\Gamma}\left(\tilde{\theta}^T\dot{\tilde{\theta}} + \tilde{\sigma}^T\dot{\tilde{\theta}}\right) \tag{3.21}$$

Consider [42] to apply projection operator

$$\dot{V}\left(\tilde{x}, \tilde{\theta}, \tilde{\sigma}\right) = \dot{\tilde{x}}^T Q\tilde{x} + 2\tilde{x}^T Pb\left(\tilde{\theta}\|x\|_\infty + \tilde{\sigma}\right) \tag{3.22}$$

$$+ 2\left(\tilde{\theta}^T \mathrm{Proj}\left(\tilde{\theta}, -\|x\|_\infty bP\tilde{x}\right) + \tilde{\sigma}^T \mathrm{Proj}(\tilde{\sigma}, -bP\tilde{x})\right)$$

$$\dot{V}\left(\tilde{x}, \tilde{\theta}, \tilde{\sigma}\right) = \dot{\tilde{x}}^T Q\tilde{x} + 2\tilde{\theta}^T\left(\|x\|_\infty bP\tilde{x} + \mathrm{Proj}\left(\tilde{\theta}, -\|x\|_\infty bP\tilde{x}\right)\right) \tag{3.23}$$

$$+ 2\tilde{\sigma}^T\left(bP\tilde{x} + \mathrm{Proj}(\tilde{\sigma}, -bP\tilde{x})\right)$$

The adaptation mechanism is expressed in equations (3.24)

$$\dot{\tilde{\theta}}(t) = \dot{\hat{\theta}}(t) = \Gamma\mathrm{Proj}\left(\tilde{\theta}, -\|x\|_\infty bP\tilde{x}\right) \tag{3.24}$$

$$\dot{\tilde{\sigma}}(t) = \dot{\hat{\sigma}}(t) = \Gamma \mathrm{Proj}(\tilde{\sigma}, -bP\tilde{x})$$

where $\Gamma \in \mathbb{R}^{+}$ is the gain of adaptation law rate, and $P = P^{T} > 0$ with $Q = Q^{T} > 0$ is the matrix solved Lyapunov equation ${A_m}^{T}P + PA_m = -Q$.

The adaptive control input is defined in Laplace transform

$$u_{ad}(s) = -\frac{C(s)}{\omega}\left(\hat{\eta}(s) - k_g r(s)\right) \tag{3.25}$$

where $k_g \triangleq -\frac{1}{(c^{T}{A_m}^{-1}b)}$, $\hat{\eta}(s)$ is the Laplace transform of $\hat{\eta}(t) \triangleq \hat{\theta}(t)\|x\|_{\infty} + \hat{\sigma}(t)$ and $r(s)$ is the Laplace transform reference $r(t)$.

$C(s)$ in equation (3.26) is the selected filter with $C(0) = \boldsymbol{I}$ where $D(s) = \frac{\boldsymbol{I}}{s}$ is strictly proper transfer function

$$C(s) \triangleq \frac{\omega k D(s)}{\boldsymbol{I} + \omega k D(s)} \tag{3.26}$$

$$C(s) \triangleq \frac{\omega k}{s\boldsymbol{I} + \omega k} \tag{3.27}$$

We can define adaptive control input of the system by substituting equation (3.26) into (3.25) expressed as

$$u_{ad}(s) = -kD(s)\left(\omega u_{ad}(s) + \hat{\eta}(s) - k_g r(s)\right) \tag{3.28}$$

3.2.3 Neuro I&I Adaptive Control

The tracking error is the gap between estimated trajectory $\bar{q}$ and desired trajectory $\bar{q}_d$ as given as follow

$$e(t) = \bar{q}_d(t) - \bar{q}(t) \tag{3.29}$$

where

$$\bar{q}_d(t) = \begin{bmatrix} x_d(t) \\ y_d(t) \end{bmatrix}$$

and

$$\bar{q}(t) = \begin{bmatrix} x(t) \\ y(t) \end{bmatrix}$$

The filtered tracking error is expressed by

$$r(t) = \dot{e} + \Gamma e \tag{3.30}$$

where Γ is PD controller and $\Gamma > 0$.

By differentiating equation (2.1), we can write the dynamics robot in term of tracking error

$$M\dot{r} = -V_m r - \tau + f + \tau_d \tag{3.31}$$

where

$$f(x) = M(q)(\ddot{q}_d - \Gamma\mathrm{e}) + V_m(q, \dot{q})(\dot{q}_d + \Gamma\mathrm{e}) + F + \tau_d \tag{3.32}$$

We apply NN to estimate $f(x)$ which e and $\bar{q}_d$ are accessible. We design the controller for the system to achieve the globally exponentially stable closed loop system.

$$\tau = \psi(x)\big(\hat{\theta}_0 + \beta_0\big) + K_f r + \delta - \Gamma \tag{3.33}$$

where $\psi(x)\hat{\theta}_0$ is the estimated $f(x)$, $\hat{\theta}_0$ is the weight of NN from adaptation law of I&I, K_f is the gain matrix and δ function of disturbance and error and Γ is positive gain.

The dynamics of nonholonomic mobile robot can be written from equation (3.31) as follow

$$M\dot{r} = -V_m r - \tau + \psi(x)\big(\hat{\theta}_0 + \beta_0\big) + \delta + \tau_d \tag{3.34}$$

$$\dot{r} = M^{-1}\psi(x)\big(\hat{\theta}_0 + \beta_0\big) - M^{-1}V_m r + M^{-1}\delta + M^{-1}\tau_d - M^{-1}\tau \tag{3.35}$$

The equation (3.20) can be written linearly parameterized system as

$$\dot{x} = \psi(x)\hat{\theta}_0 + f_1 + Gu \tag{3.36}$$

where

$$r \triangleq x \qquad \tau \triangleq u \qquad G \triangleq -M^{-1}$$

$$f_1 = -M^{-1}V_m r + M^{-1}\delta + M^{-1}\tau_d \tag{3.37}$$

To apply I&I adaptive control on the rotational dynamics, define the following implicit manifold

$$z_0 = \hat{\theta}_0 - \theta_0 + \beta_0(x) \tag{3.38}$$

and the dynamic system is expressed by

$$\dot{z}_0 = \dot{\hat{\theta}}_0 + \frac{\partial \beta_0}{\partial x}\dot{x}$$

$$\dot{z}_0 = \dot{\hat{\theta}}_0 + \frac{\partial \beta_0}{\partial x}(\psi(x)\theta_0 + f_1 + Gu) \tag{3.39}$$

The adaptation law is selected as

$$\dot{\hat{\theta}}_0 = -\frac{\partial \beta_0(x)}{\partial x}\left(\psi(x)\left(\hat{\theta}_0 + \beta_0\right) + f_1 + Gu\right) \tag{3.40}$$

The dynamics of nonholonomic mobile robot in term of tracking error is equal to

$$M\dot{r} = -V_m r - k_a r - \psi(x)\left(\hat{\theta}_0 + \beta_0\right) + \psi(x)\theta_0 + \delta + \tau_d - \Gamma \tag{3.41}$$

where k_a and Γ are positive gain to bring the system to zero manifold.

$$M\dot{r} = kr - \psi(x)\tilde{\theta}_0 + \psi(x)\beta_0 + \delta + \tau_d - \Gamma \tag{3.42}$$

where $k = V_m + k_a$

$$M\dot{r} = kr - \psi(x)z + \delta + \tau_d - \Gamma \tag{3.43}$$

We apply Lyapunov stability theorem to define the stability condition of the system

$$V = \frac{1}{2}z^T z + \frac{1}{2}\tilde{\theta}_0{}^T\tilde{\theta}_0 + \frac{1}{2}x^T M \tag{3.44}$$

$$V = V_1 + V_2 + V_3 \tag{3.45}$$

$$\dot{V} = \dot{V}_1 + \dot{V}_2 + \dot{V}_3 \tag{3.46}$$

Assume $\delta = 0$ and $\Gamma = 0$. Let $\dot{\tilde{\theta}}_0 = M^{-1}kx$, then

$$\dot{V}_1 = -z^T\left[\frac{\partial \beta_0}{\partial x}M^{-1}k\psi(x)\right]z + z^T\frac{\partial \beta_0}{\partial x}M^{-1}[\delta - \Gamma] \tag{3.47}$$

$$\dot{V}_2 = \tilde{\theta}_0{}^T \frac{\partial \beta_0}{\partial x} M^{-1} kx + x^T k^T M^{-1} \left[\frac{\partial \beta_0}{\partial x}\right]^T \tilde{\theta}_0 \tag{3.48}$$

$$\dot{V}_3 = -x^T kx - x^T \psi(x)\tilde{\theta}_0 - x^T \psi(x)\beta_0(x) \tag{3.49}$$

3.3 Quadrotor UAV

The control strategies based on I&I and L1 adaptive for trajectory tracking of single quadrotor UAV was developed by [41]. They applied cascaded control method with PD as outer loop and I&I and L1 adaptive as inner loop that we can see in figure 3.1

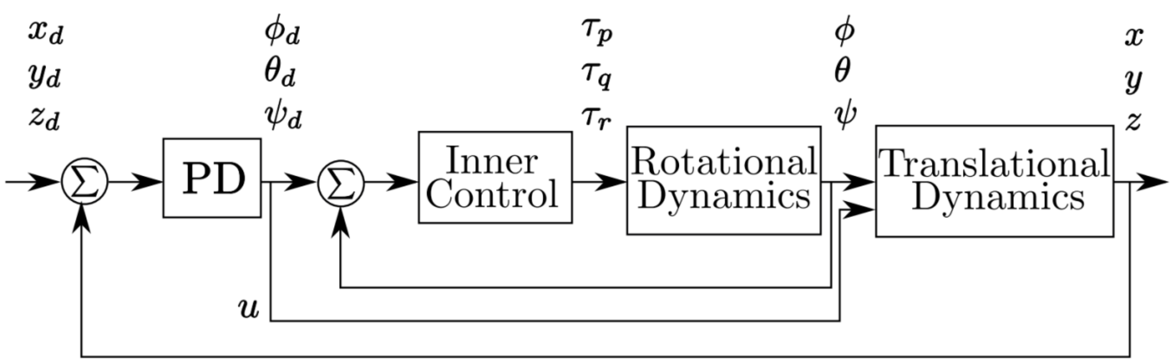

Figure 3.3 Control structure of single quadrotor UAV [41]

3.3.1 Design of I&I Adaptive Control

The linearly parameterized dynamic model of the given nonholonomic system in equation (2.31) can be written as:

$$\dot{x} = f_0(x)\theta_0 + f_1(x)\theta_1 + f_2(x)\theta_2 + f_3(x)\theta_3 + Gu \tag{3.50}$$

where

$$x \triangleq \upsilon_2, \qquad G \triangleq diag\left({I_x}^{-1}, {I_y}^{-1}, {I_z}^{-1}\right), \quad u = \left[\tau_p,\ \tau_q,\ \tau_r\right]^T,$$

$$\theta_0 \triangleq [I_1, I_2, I_3]^T, \qquad \theta_1 \triangleq I_R\Omega, \qquad \theta_2 \triangleq -I_R\Omega, \quad \theta_3 \triangleq -I_R,$$

$$f_0(x) \triangleq diag(-qr, -pr, -pq), \qquad f_1(x) \triangleq [q, 0, 0]^T,$$

$$f_2(x) \triangleq [0, p, 0]^T, \qquad f_3(x) \triangleq [p, q, r]^T$$

$$I_1 = \frac{I_z - I_y}{I_x}, \qquad I_2 = \frac{I_x - I_z}{I_y}, \qquad I_3 = \frac{I_y - I_x}{I_z},$$

Equation (3.51) is the selected controller

$$u = G^{-1}(-f_0\theta_0 - f_1\theta_1 - f_2\theta_2 - f_3\theta_3 - K_B x + K_F r) \tag{3.51}$$

where $K_F > 0$ is the feedforward gain, feedback gain $K_B > 0$ and r is the reference system.

In order to achieve the globally exponentially stable closed loop system we apply feedforward and feedback gains as

$$\dot{x} = -K_B x + K_F r \tag{3.52}$$

To apply I&I adaptive control on the rotational dynamics, define the following implicit manifold

$$z_0 = \hat{\theta}_0 - \theta_0 + \beta_0(x) \tag{3.53}$$

$$z_i = \hat{\theta}_i - \theta_i + \beta_i(x), \qquad i = 1, 2, 3$$

and the dynamic system is expressed by

$$\dot{z}_0 = \dot{\hat{\theta}}_0 + \frac{\partial \beta_0}{\partial x}\dot{x}$$

$$\dot{z}_0 = \dot{\hat{\theta}}_0 + \frac{\partial \beta_0}{\partial x}(f_0(x)\theta_0 + f_1(x)\theta_1 + f_2(x)\theta_2 + f_3(x)\theta_3 + Gu) \tag{3.54}$$

$$\dot{z}_i = \dot{\hat{\theta}}_i + \frac{\partial \beta_i}{\partial x}\dot{x}$$

$$\dot{z}_i = \dot{\hat{\theta}}_i + \frac{\partial \beta_i}{\partial x}(f_0(x)\theta_0 + f_1(x)\theta_1 + f_2(x)\theta_2 + f_3(x)\theta_3 + Gu) \tag{3.55}$$

The adaptation law $\left(\omega\left(x, \hat{\theta}_l\right) = \dot{\hat{\theta}}_l\right)$ is selected as

$$\omega_0 = -\frac{\partial \beta_0(x)}{\partial x}\Big(f_0(x)\left(\hat{\theta}_0 + \beta_0\right) + f_1(v)\left(\hat{\theta}_1 + \beta_1 - z_1\right) + f_2(v)\left(\hat{\theta}_2 + \beta_2 - z_2\right) + f_3(v)\left(\hat{\theta}_3 + \beta_3 - z_3\right) + Gu\Big) \tag{3.56}$$

$$\omega_1 = -\frac{\partial \beta_1(x)}{\partial x}\Big(f_0(x)\left(\hat{\theta}_0 + \beta_0 - z_0\right) + f_1(v)\left(\hat{\theta}_1 + \beta_1 - z_1\right) + f_2(v)\left(\hat{\theta}_2 + \beta_2 - z_2\right) + f_3(v)\left(\hat{\theta}_3 + \beta_3 - z_3\right) + Gu\Big) \tag{3.57}$$

$$\omega_2 = -\frac{\partial \beta_2(x)}{\partial x}\Big(f_0(x)\left(\hat{\theta}_0 + \beta_0 - z_0\right) + f_1(v)\left(\hat{\theta}_1 + \beta_1 - z_1\right) + f_2(v)\left(\hat{\theta}_2 + \beta_2 - z_2\right) + f_3(v)\left(\hat{\theta}_3 + \beta_3 - z_3\right) + Gu\Big) \tag{3.58}$$

$$\omega_3 = -\frac{\partial \beta_3(x)}{\partial x}\Big(f_0(x)\left(\hat{\theta}_0 + \beta_0 - z_0\right) + f_1(v)\left(\hat{\theta}_1 + \beta_1 - z_1\right) + f_2(v)\left(\hat{\theta}_2 + \beta_2 - z_2\right) + f_3(v)\left(\hat{\theta}_3 + \beta_3 - z_3\right) + Gu\Big) \tag{3.59}$$

substituting these into (3.54) and (3.55), and utilizing (3.53) one will achieve

$$\dot{z}_0 = -\left(\frac{\partial \beta_0(x)}{\partial x} f_0(x)\right) z_0$$

$$\dot{z}_i = -\left(\frac{\partial \beta_i(x)}{\partial x} f_i(x)\right) z_i \tag{3.60}$$

$\frac{\partial \beta_0(v)}{\partial v} = \gamma_0 {f_0}^T(v)$, where $\gamma_0 > 0$ is selected, the following is obtained

$$\lim_{n\to\infty} z(t) = 0 \qquad \Rightarrow \qquad \theta_l = \hat{\theta}_l + \beta\,(x) \tag{3.61}$$

The I&I adaptive control is expressed by

$$u = G^{-1}\big(-f_0(\hat{\theta}_0 + \beta_0) - f_1(\hat{\theta}_1 + \beta_1) - f_2(\hat{\theta}_2 + \beta_2) - f_3(\hat{\theta}_3 + \beta_3) - K_B v + K_F r\big) \tag{3.62}$$

3.3.2 Design of L1Adaptive Control

The linearly parameterized rotational dynamics of quadrotor UAV in Equation (2.31) can be rewritten as,

$$\dot{x}(t) = A_m x(t) + b\left(f\big(t, x(t)\big) + \omega u_{ad}(t)\right) \tag{3.63}$$

$$x(0) = x_0 \qquad\qquad y(t) = c^T x(t)$$

where

$x \triangleq v_2, \qquad A_m \in \mathbb{R}^{n\times n} \triangleq$ a known a desired Hurwitz matrix

$$b = 1, \qquad \omega = {I_M}^{-1}, \qquad u_{ad} \triangleq \tau \triangleq \mathcal{L}_1 \text{adaptive control,}$$

$$f\big(t, x(t)\big) \triangleq {I_M}^{-1}(-(v_2 \times I_M v_2) - I_R(v_2 - z_e)\Omega - k_r v_2), \; c^T = I_{3\times3} \tag{3.64}$$

Equation (2.31) can be rewritten as

$$\dot{x}(t) = A_m x(t) + b(\omega u_{ad} + \theta \|x\|_\infty + \sigma) \tag{3.65}$$

$$x(0) = x_0 \qquad y(t) = c^T x(t)$$

Let consider state predictor as linearly parameterized system in (3.48) as

$$\dot{\hat{x}}(t) = A_m \hat{x}(t) + b\big(\omega u_{ad} + \hat{\theta} \|x\|_\infty + \hat{\sigma}\big) \tag{3.66}$$

$$\hat{x}(0) = x_0 \qquad \hat{y}(t) = c^T \hat{x}(t)$$

where $\hat{x}(t) \in \mathbb{R}^n$ is state of the predictor, $\hat{y}(t) \in \mathbb{R}^n$ is predicted output and $\hat{\theta}$ and $\hat{\sigma}$ are estimation of θ and σ respectively.

We define error dynamic of the system as

$$\dot{\tilde{x}}(t) = A_m \tilde{x}(t) + b\big(\omega u_{ad} + \tilde{\theta} \|x\|_\infty + \tilde{\sigma}\big), \qquad \tilde{x}(0) = x_0 \tag{3.67}$$

where the errors are equal to $\tilde{x}(t) \triangleq \hat{x}(t) - x(t)$, $\tilde{\theta}(t) \triangleq \hat{\theta}(t) - \theta(t)$ and $\tilde{\sigma}(t) \triangleq \hat{\sigma}(t) - \sigma(t)$.

We apply Lyapunov function to define the stability condition of the system

$$V\big(\tilde{x}, \tilde{\theta}, \tilde{\sigma}\big) = \tilde{x}^T P \tilde{x} + \frac{1}{\Gamma}\big(\tilde{\theta}^T \tilde{\theta} + \tilde{\sigma}^T \tilde{\sigma}\big) \tag{3.68}$$

Equation (3.63) is the derivative of Lyapunov candidate

$$\dot{V}\left(\tilde{x},\tilde{\theta},\tilde{\sigma}\right)=\dot{\tilde{x}}^{T}P\tilde{x}+\tilde{x}^{T}P\dot{\tilde{x}}+\frac{2}{\Gamma}\left(\tilde{\theta}^{T}\dot{\tilde{\theta}}+\tilde{\sigma}^{T}\dot{\tilde{\theta}}\right) \tag{3.69}$$

$$\dot{V}\left(\tilde{x},\tilde{\theta},\tilde{\sigma}\right)=-\tilde{x}^{T}P\tilde{x}+2\tilde{x}^{T}Pb\left(\tilde{\theta}\|x\|_{\infty}+\tilde{\sigma}\right)+\frac{2}{\Gamma}\left(\tilde{\theta}^{T}\dot{\tilde{\theta}}+\tilde{\sigma}^{T}\dot{\tilde{\theta}}\right) \tag{3.70}$$

Consider [42] to apply projection operator

$$\dot{V}\left(\tilde{x},\tilde{\theta},\tilde{\sigma}\right)=\dot{\tilde{x}}^{T}Q\tilde{x}+2\tilde{x}^{T}Pb\left(\tilde{\theta}\|x\|_{\infty}+\tilde{\sigma}\right) \tag{3.71}$$

$$+\,2\left(\tilde{\theta}^{T}\mathrm{Proj}\left(\tilde{\theta},-\|x\|_{\infty}bP\tilde{x}\right)+\tilde{\sigma}^{T}\mathrm{Proj}(\tilde{\sigma},-bP\tilde{x})\right)$$

$$\dot{V}\left(\tilde{x},\tilde{\theta},\tilde{\sigma}\right)=\dot{\tilde{x}}^{T}Q\tilde{x}+2\tilde{\theta}^{T}\left(\|x\|_{\infty}bP\tilde{x}+\mathrm{Proj}\left(\tilde{\theta},-\|x\|_{\infty}bP\tilde{x}\right)\right) \tag{3.72}$$

$$+\,2\tilde{\sigma}^{T}\left(bP\tilde{x}+\mathrm{Proj}(\tilde{\sigma},-bP\tilde{x})\right)$$

The adaptation mechanism is expressed in equations (3.73)

$$\dot{\tilde{\theta}}(t)=\dot{\hat{\theta}}(t)=\Gamma\mathrm{Proj}\left(\tilde{\theta},-\|x\|_{\infty}bP\tilde{x}\right) \tag{3.73}$$

$$\dot{\tilde{\sigma}}(t)=\dot{\hat{\sigma}}(t)=\Gamma\mathrm{Proj}(\tilde{\sigma},-bP\tilde{x})$$

where $\Gamma\in\mathbb{R}^{+}$ is the gain of adaptation law rate, and $P=P^{T}>0$ with $Q=Q^{T}>0$ is the matrix solved Lyapunov equation ${A_m}^{T}P+PA_m=-Q$.

The adaptive control input is defined in Laplace transform

$$u_{ad}(s)=-\frac{C(s)}{\omega}\left(\hat{\eta}(s)-k_{g}r(s)\right) \tag{3.74}$$

where $k_g\triangleq-\frac{1}{(c^{T}{A_m}^{-1}b)}$, $\hat{\eta}(s)$ is the Laplace transform of $\hat{\eta}(t)\triangleq\hat{\theta}(t)\|x\|_{\infty}+\hat{\sigma}(t)$ and $r(s)$ is the Laplace transform reference $r(t)$.

$C(s)$ in equation (3.58) is the selected filter with $C(0) = \boldsymbol{I}$ where $D(s) = \frac{\boldsymbol{I}}{s}$ is strictly proper transfer function

$$C(s) \triangleq \frac{\omega k D(s)}{\boldsymbol{I} + \omega k D(s)} \tag{3.75}$$

$$C(s) \triangleq \frac{\omega k}{s\boldsymbol{I} + \omega k} \tag{3.76}$$

We can define adaptive control input of the system by substituting equation (3.75) into (3.74) as

$$u_{ad}(s) = -kD(s)\left(\omega u_{ad}(s) + \hat{\eta}(s) - k_g r(s)\right) \tag{3.77}$$

CHAPTER 4

COOPERATIVE CONTROL DESIGN

4.1 Introduction

This chapter deals with cooperative control design for heterogeneous systems based on potential field. In this study we consider the cooperative control of nonholonomic mobile robot and quadrotor UAV moving together in one formation. We adopt the concept of cooperative control based on potential field from [40] and [43].

4.2 Shape Formation

Let the sensing range of each robot assumed to be S_r as shown in figure 5.1, and each robot can access the position of its neighbors that are present within the sensing range. All robots present in the fleet are required to move in a particular polygon. These robots are localized around a moving leader. The distance between each two neighboring agents should be equal to $L \leq S_r$. The circumcircle of the desired polygon has a radius of r. $x_c \in R^2$ is the coordinate of the moving leader which is generated by potential field approach on the group leader. From the basic geometry, r will be [33]

$$r = \frac{L}{2sin(\pi/n)} \tag{4.1}$$

where n is number of agents.

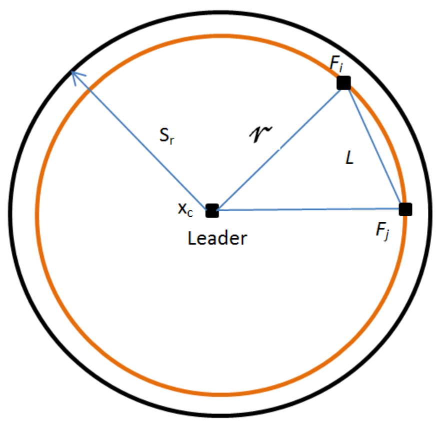

Figure 4.1 The leader sensing range $\mathbf{F_i}$, $\mathbf{F_j}$ followers.

We define EL as the error of the formation control about desired L (L_d) in percentage (%) and ER as the error of the formation control about desired r (r_d) in percentage (%) as follows

$$EL = \frac{|L - L_d|}{L_d} \times 100\% \tag{4.2}$$

$$ER = \frac{|r - r_d|}{r_d} \times 100\% \tag{4.3}$$

4.3 Control Design

The formation control based on the attractive and repulsive potential of the agent is applied in this thesis. Equation (4.4) express the cooperative control of multi-agent systems

$$u_i = P_{ce} + P_{ij} + Da \tag{4.4}$$

where:

P_{ce}: The center potential

P_{ij}: The inter-agent potential (agent's potential)

Da: Damping action

The adaptive cooperative control scheme of heterogeneous systems based on I&I and L1 adaptive control illustrates in figure 4.2. In potential field control, the center potential attracts each agent to the center while the inter-agent potential repulses two neighboring agents to avoid collision. We consider x, y, θ as nonholonomic mobile robot and x, y, z, θ as quadrotor UAV orientation with respect to the inertial frame respectively. For each agent, we apply cascaded control where PD is the controller of outer loop and I&I and L1 as controller of inner loop.

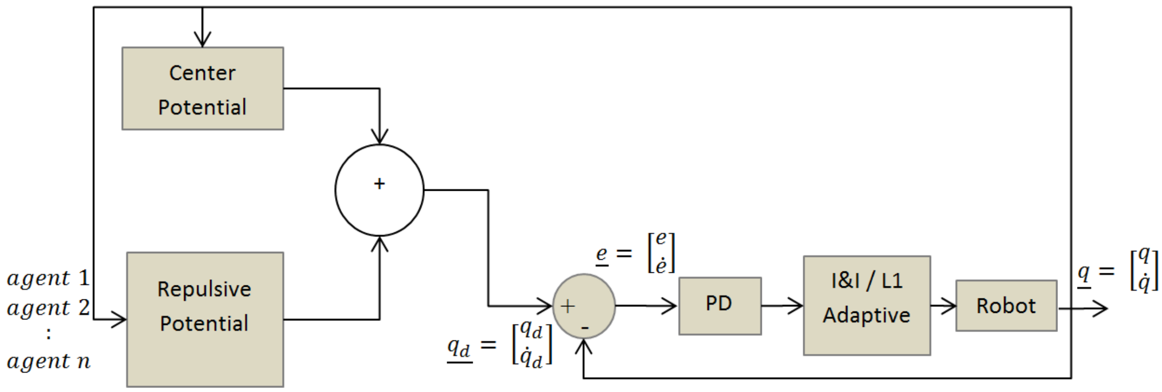

Figure 4.2 The scheme of adaptive cooperative control of heterogeneous systems

Figure 4.3 shows the adaptive cooperative control scheme of nonholonomic mobile robot based on neuro I&I. In potential field control, the center potential attracts each agent to the center while the inter-agent potential repulses two neighboring agents to avoid collision. We consider x, y, θ as nonholonomic mobile as nonholonomic mobile robot orientation with respect to the inertial frame. For each agent, we apply tracking error position to generate required input of NN. NN compute the nonlinearity of dynamics, and then I&I adaptive compute the weight of NN.

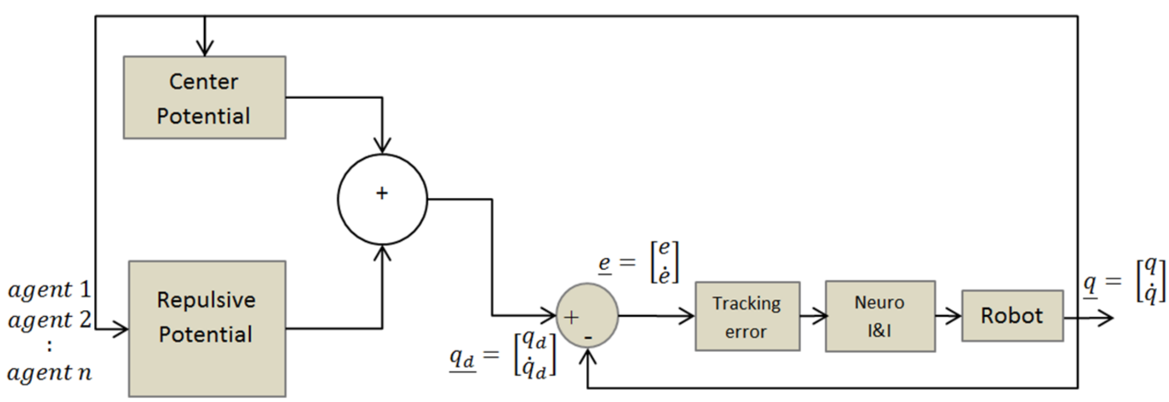

Figure 4.3 The scheme of adaptive cooperative control of nonholonomic mobile robot based on neuro I&I

4.4 Cooperative Control of Nonholonomic Mobile Robot

4.4.1 Center Potential

Let us first start with defining the center potential of nonholonomic mobile robot as

$$P_{att} = -\nabla_{P_i} V_{C_i}(P_i) \tag{4.5}$$

where

$$V_{C_i} = \frac{1}{2} K_c (R_{C_i} - r)^2 \tag{4.6}$$

$$P_i = \lfloor x_i \quad y_i \quad \theta_i \rfloor^T$$

$$P_c = \lfloor x_c \quad y_c \quad \theta_c \rfloor^T$$

where R_{C_i} is the distance between leader and agent i that can be calculated as

$$R_{C_i} = \sqrt{(x_i - x_c)^2 + (y_i - y_c)^2 + (\theta_i - \theta_c)^2} \tag{4.7}$$

Now calculating the time derivative of V_{C_i} given in equation (4.6) with respect to P_i we obtain the center potential between the follower i and the center robot. The steps involved in this differentiation is shown as

$$P_{att} = -\left(\frac{\partial V_{C_i}}{\partial R_{C_i}}\right)\left(\frac{\partial R_{C_i}}{\partial P_i}\right) \tag{4.8}$$

Now the time derivative of V_{C_i} with respect to R_{C_i} is given by,

$$\left(\frac{\partial V_{C_i}}{\partial R_{C_i}}\right) = K_c\left(R_{C_i} - r\right) \tag{4.9}$$

if

$$D = (x_i - x_c)^2 + (y_i - y_c)^2 + (\theta_i - \theta_c)^2 \tag{4.10}$$

then

$$R_{C_i} = D^{\frac{1}{2}} \tag{4.11}$$

Let us implement the chain rule and differentiate R_{C_i} with respect to P_i as

$$\frac{\partial R_{C_i}}{\partial P_i} = \frac{\partial R_{C_i}}{\partial D}\frac{\partial D}{\partial P_i} \tag{4.12}$$

where from (4.11) we have

$$\frac{\partial R_{C_i}}{\partial D} = \frac{1}{2}D^{-\frac{1}{2}} \tag{4.13}$$

and

$$\frac{\partial D}{\partial P_i} = \frac{\partial D}{\partial x_i} + \frac{\partial D}{\partial y_i} + \frac{\partial D}{\partial \theta_i} \tag{4.14}$$

$$\frac{\partial D}{\partial P_i} = 2(x_i - x_c) + 2(y_i - y_c) + 2(\theta_i - \theta_c) \tag{4.15}$$

$$\frac{\partial D}{\partial P_i} = 2(P_i - P_c)^T \tag{4.16}$$

By substituting (4.13) and (4.16) into (4.12) we will get

$$\frac{\partial R_{C_i}}{\partial P_i} = \frac{1}{2}D^{-\frac{1}{2}}2(P_i - P_c)^T = \frac{1}{R_{C_i}}(P_i - P_c)^T \tag{4.17}$$

The attractive potential between each agent to the center of robot is calculated by substituting (4.17) and (4.9) into (4.8) as

$$P_{att} = \frac{1}{R_{c_i}}\left[K_c\left(R_{c_i} - r\right)\right][P_i(t) - P_c(t)]^T \tag{4.18}$$

where

K_c : a positive constant

r : the circumcircle radius of the desired polygon

4.4.2 Inter-agents Potential

The repulsive potential between two neighboring agents i and j is expressed by

$$P_{ij} = -\nabla_{P_i} V_{ij}(P_i, P_j) \tag{4.19}$$

where

$$V_{ij} = \begin{cases} \frac{1}{2} K_a \left(R_{ij} - L\right)^2, & R_{f_i} < 0 \\ 0, & otherwise \end{cases} \tag{4.20}$$

and

$$P_j = \lfloor x_j \quad y_j \quad \theta_j \rfloor^T$$

where R_{f_i} is the distance between two neighboring agents that can be calculated as

$$R_{f_i} = \sqrt{(x_i - x_c)^2 + (y_i - y_c)^2 + (\theta_i - \theta_c)^2} \tag{4.21}$$

The repulsive potential between two neighboring agent i and j is expressed by

$$P_{rep} = -K_a\left(R_{f_i} - L\right)\frac{1}{R_{f_i}}\left[\left(P_i(t) - P_j(t)\right)^T - \left(P_j(t) - P_i(t)\right)^T\right] \tag{4.22}$$

where

K_a : a positive constant

R_{f_i} : distance between two neighboring agents

L : distance between each two neighboring followers

4.5 Cooperative Control of Quadrotor UAV

4.5.1 Center Potential

Let us first start with defining the center potential of nonholonomic mobile robot as

$$P_{att} = -\nabla_{P_i} V_{C_i}(P_i) \tag{4.23}$$

where

$$V_{C_i} = \frac{1}{2} K_c (R_{C_i} - r)^2 \tag{4.24}$$

and

$$P_i = \lfloor x_i \quad y_i \quad z_i \quad \theta_i \rfloor^T$$

$$P_c = \lfloor x_c \quad y_c \quad z_c \quad \theta_c \rfloor^T$$

where R_{C_i} is the distance between leader and agent i that can be calculated as

$$R_{C_i} = \sqrt{(x_i - x_c)^2 + (y_i - y_c)^2 + (z_i - z_c)^2 + (\theta_i - \theta_c)^2} \tag{4.25}$$

Now calculating the time derivative of V_{C_i} given in equation (4.24) with respect to P_i we obtain the center potential between the follower i and the center robot. The steps involved in this differentiation is shown as

$$P_{att} = -\left(\frac{\partial V_{C_i}}{\partial R_{C_i}}\right)\left(\frac{\partial R_{C_i}}{\partial P_i}\right) \tag{4.26}$$

Now the time derivative of V_{C_i} with respect to R_{C_i} is given by,

$$\left(\frac{\partial V_{C_i}}{\partial R_{C_i}}\right) = K_c\left(R_{C_i} - r\right) \tag{4.27}$$

if

$$D = (x_i - x_c)^2 + (y_i - y_c)^2 + (z_i - z_c)^2 + (\theta_i - \theta_c)^2 \tag{4.29}$$

then

$$R_{C_i} = D^{\frac{1}{2}} \tag{4.30}$$

Let us implement the chain rule and differentiate R_{C_i} with respect to P_i as

$$\frac{\partial R_{C_i}}{\partial P_i} = \frac{\partial R_{C_i}}{\partial D}\frac{\partial D}{\partial P_i} \tag{4.31}$$

where from (4.29) we have

$$\frac{\partial R_{C_i}}{\partial D} = \frac{1}{2}D^{-\frac{1}{2}} \tag{4.32}$$

and

$$\frac{\partial D}{\partial P_i} = \frac{\partial D}{\partial x_i} + \frac{\partial D}{\partial y_i} + \frac{\partial D}{\partial z_i} + \frac{\partial D}{\partial \theta_i} \tag{4.33}$$

$$\frac{\partial D}{\partial P_i} = 2(x_i - x_c) + 2(y_i - y_c) + 2(z_i - z_c) + 2(\theta_i - \theta_c) \tag{4.34}$$

$$\frac{\partial D}{\partial P_i} = 2(P_i - P_c)^T \tag{4.35}$$

By substituting (4.32) and (4.35) into (4.30) we will get

$$\frac{\partial R_{C_i}}{\partial P_i} = \frac{1}{2}D^{-\frac{1}{2}}2(P_i - P_c)^T = \frac{1}{R_{C_i}}(P_i - P_c)^T \tag{4.36}$$

The attractive potential between each agent to the center of robot is calculated by substituting (4.36) and (4.27) into (4.26) as

$$P_{att} = \frac{1}{R_{c_i}}\left[K_c\left(R_{c_i} - r\right)\right][P_i(t) - P_c(t)]^T \tag{4.37}$$

where

K_c : a positive constant

r : the circumcircle radius of the desired polygon

4.5.2 Inter-agents Potential

The repulsive potential between two neighboring agents i and j is expressed by

$$P_{ij} = -\nabla_{P_i} V_{ij}(P_i, P_j) \tag{4.38}$$

where

$$V_{ij} = \begin{cases} \frac{1}{2} K_a\left(R_{ij} - L\right)^2, & R_{f_i} < 0 \\ 0, & otherwise \end{cases} \tag{4.39}$$

and

$$P_j = \left\lfloor x_j \quad y_j \quad z_j \quad \theta_j \right\rfloor^T$$

where R_{f_i} is the distance between two neighboring agents that can be calculated as

$$R_{f_i} = \sqrt{(x_i - x_c)^2 + (y_i - y_c)^2 + (z_i - z_c)^2 + (\theta_i - \theta_c)^2} \tag{4.40}$$

The repulsive potential between two neighboring agent i and j is expressed by

$$P_{rep} = -K_a\left(R_{f_i} - L\right)\frac{1}{R_{f_i}}\left[\left(P_i(t) - P_j(t)\right)^T - \left(P_j(t) - P_i(t)\right)^T\right] \tag{4.41}$$

where

K_a : a positive constant

R_{f_i} : distance between two neighboring agents

L : distance between each two neighboring followers

CHAPTER 5

SIMULATION RESULTS

5.1 Introduction

In this chapter the effectiveness of the proposed adaptive cooperative control schemes are investigated based on I&I and L1 control techniques. Later, the results of both the control techniques are compared for heterogeneous systems. This chapter also presents the I&I, L1 and neuro I&I approaches for adaptive cooperative control of nonholonomic mobile robots to follow the desired formation.

5.2 Adaptive Cooperative Control of Heterogeneous Systems

In this section we will discuss two cases; case 1 when the leader of the heterogeneous systems move in x direction, and in case 2 the leader of the heterogeneous systems move in x as well as y direction. The heterogenous systems here consists of 3 agents, where first agent is quadrotor UAV, followed by agent 2 and 3 which are nonholonomic mobile robots surrounded by the leader in the center. The desired distance for each agent is 1.5 for both case 1 and case 1

Figure (5.1-5.8) show the comparison of I&I and L1 performance for adaptive cooperative control of heterogeneous systems. In this first case, both controllers, I&I and L1 adaptive are able to navigate the heterogeneous robots and follow the leader in group formation on unknown maps.

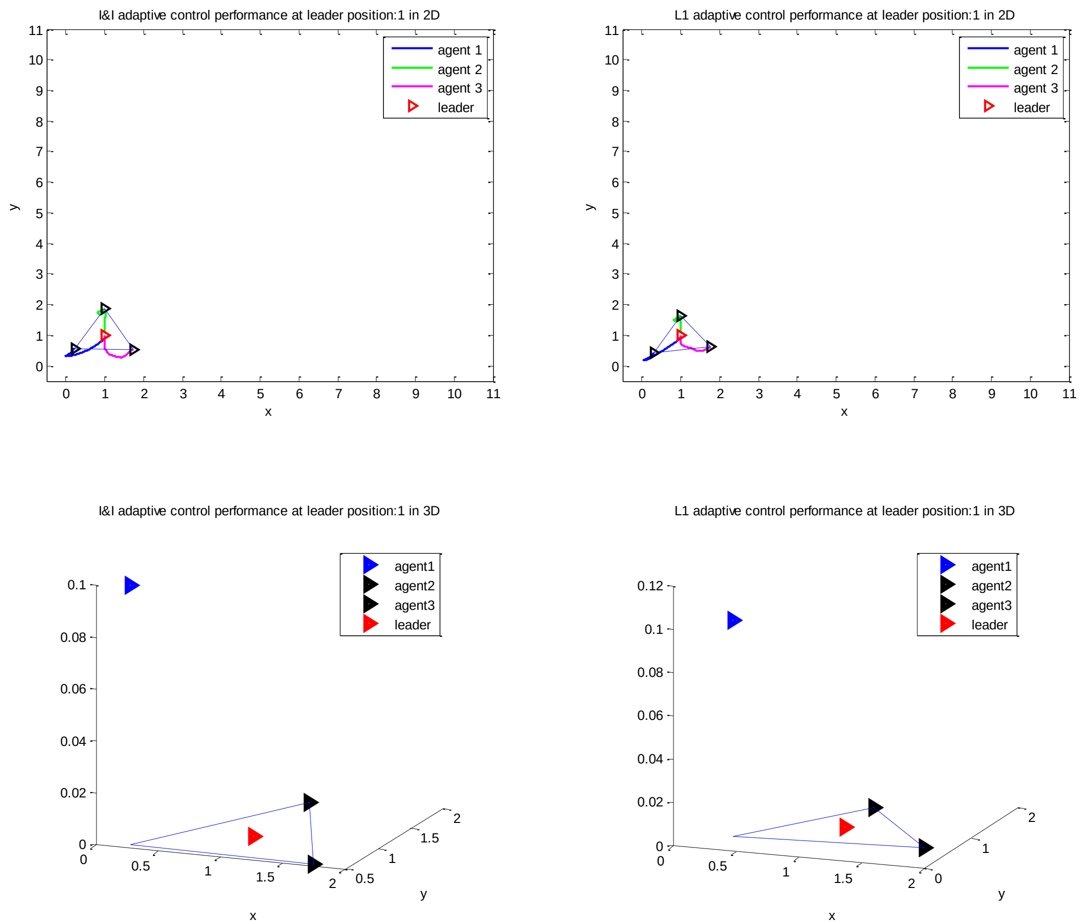

Figure 5.1 The group formation when the leader is at position $(\mathbf{1}, \mathbf{1})$.

Figure 5.1 shows the first agent move from (1.02, 1), second agent from (1, 1.08) and third agent from (1, 0.99) respectively to follow the leader at (1, 1). We can see the ability of I&I and L1 adaptive controllers to navigate each agent to track the desired formation.

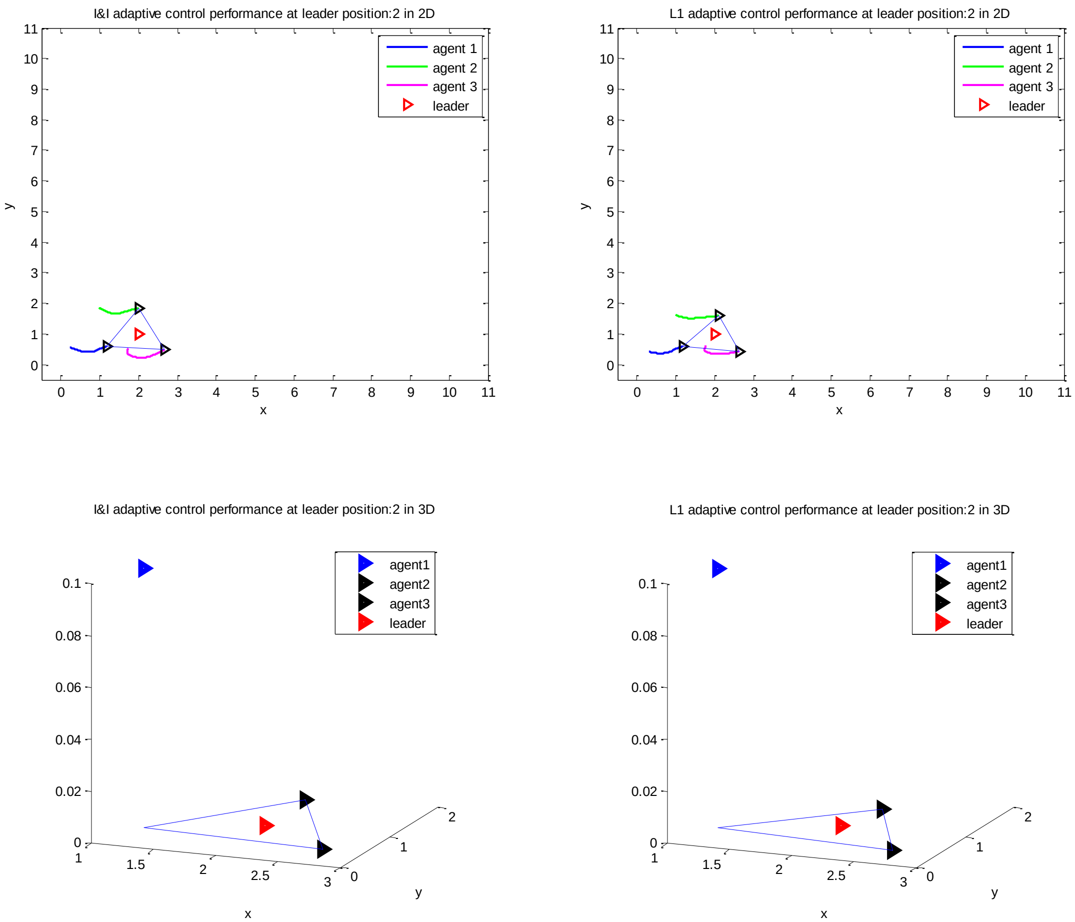

Figure 5.2 The group formation when the leader is at position $(\mathbf{2}, \mathbf{1})$.

Figure 5.2 shows the each agent move from position 1 to follow the leader at (2, 1). We can see the ability of I&I and L1 adaptive controllers to navigate each agent to track the desired formation.

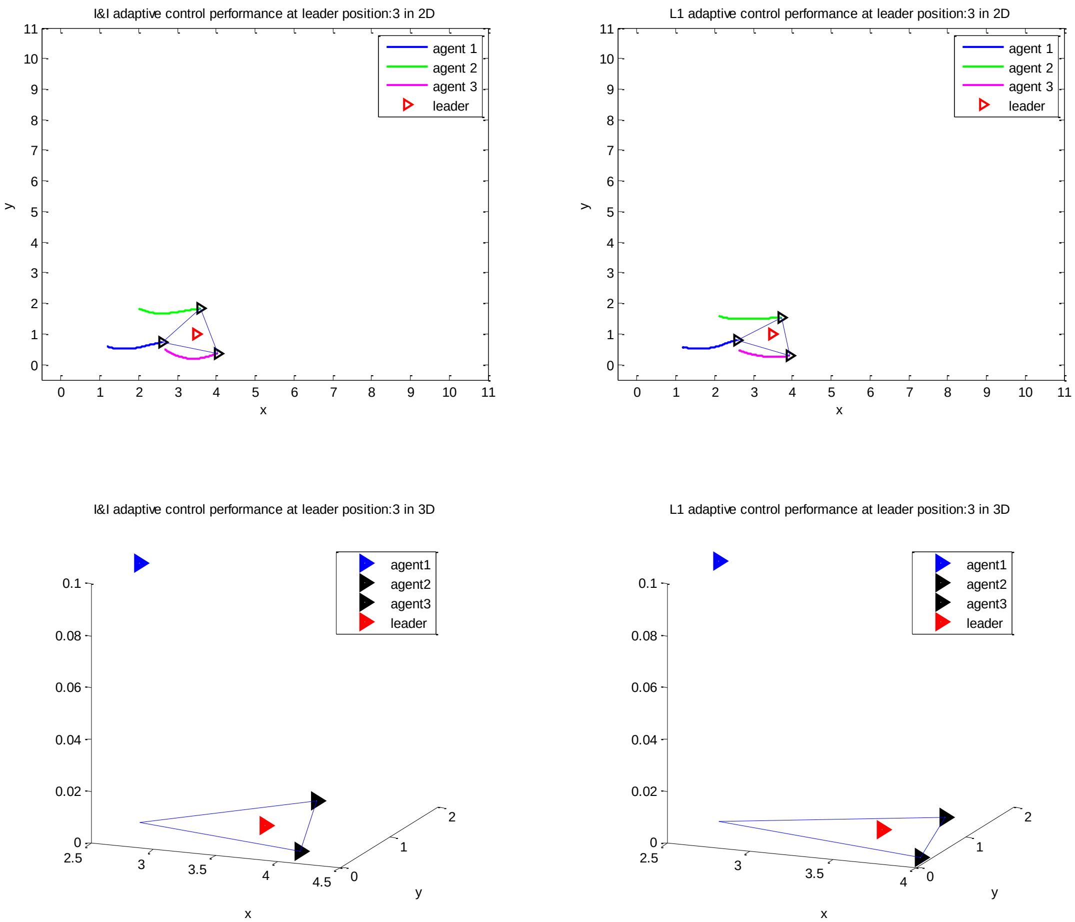

Figure 5.3 The group formation when the leader is at position $(\mathbf{3.5, 1})$.

Figure 5.3 shows the each agent move from position 2 to follow the leader at (3.5, 1). We can see the ability of I&I and L1 adaptive controllers to navigate each agent to track the desired formation.

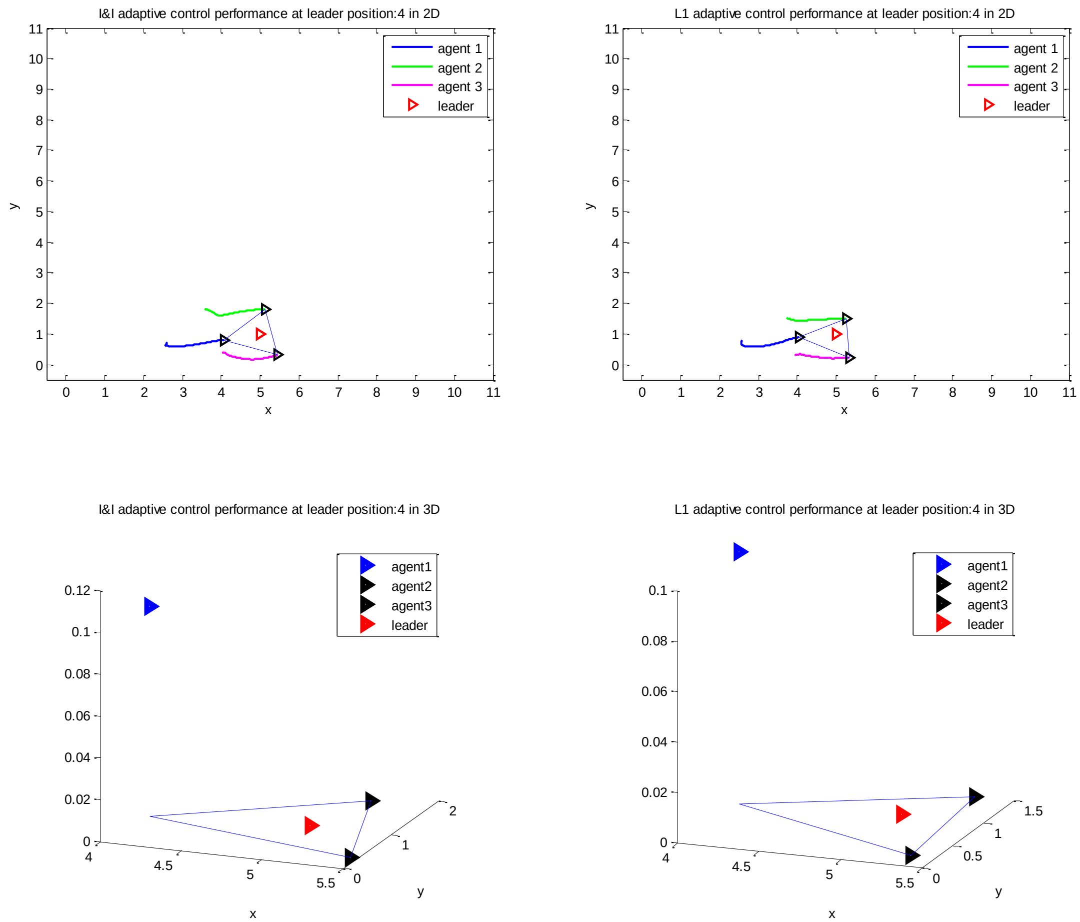

Figure 5.4 The group formation when the leader is at position $(\mathbf{5}, \mathbf{1})$.

Figure 5.4 shows the each agent move from position 3 to follow the leader at (5, 1). We can see the ability of I&I and L1 adaptive controllers to navigate each agent to track the desired formation.

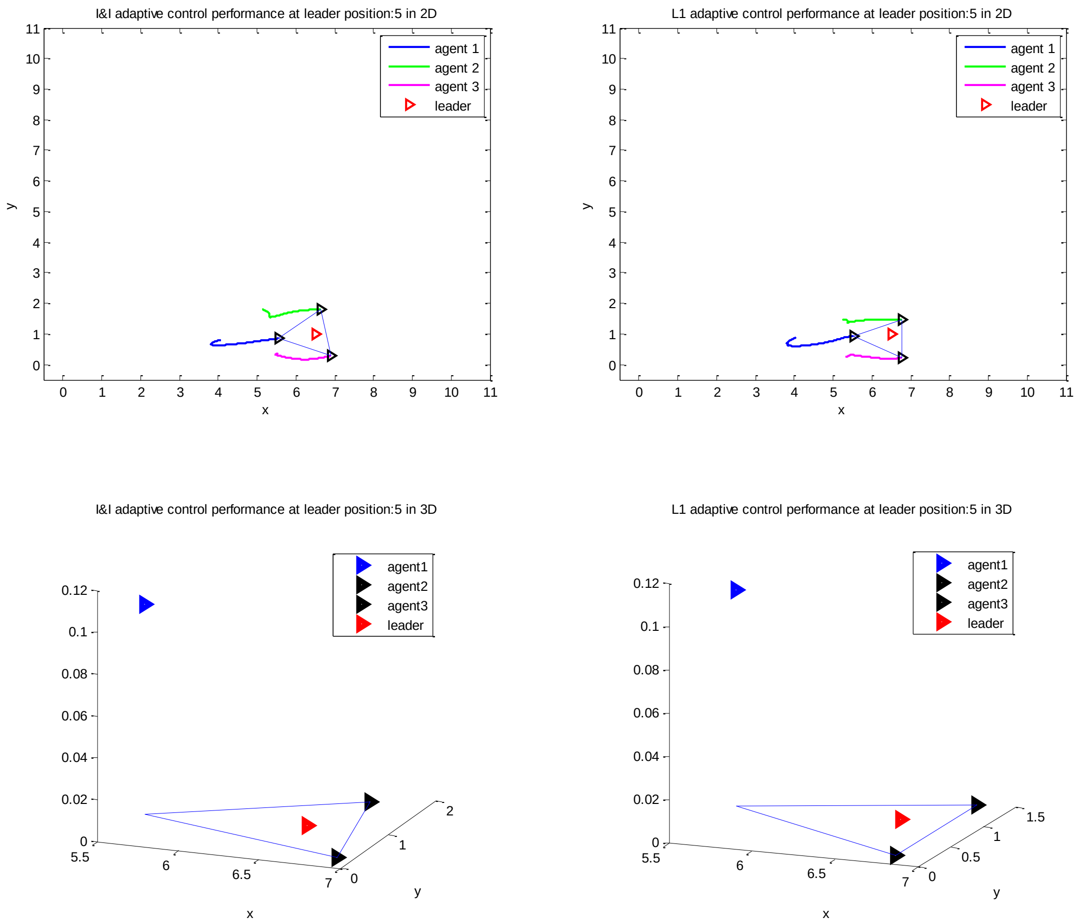

Figure 5.5 The group formation when the leader is at position $(\mathbf{6.5}, \mathbf{1})$.

Figure 5.5 shows the each agent move from position 4 to follow the leader at (6.5, 1). We can see the ability of I&I and L1 adaptive controllers to navigate each agent to track the desired formation.

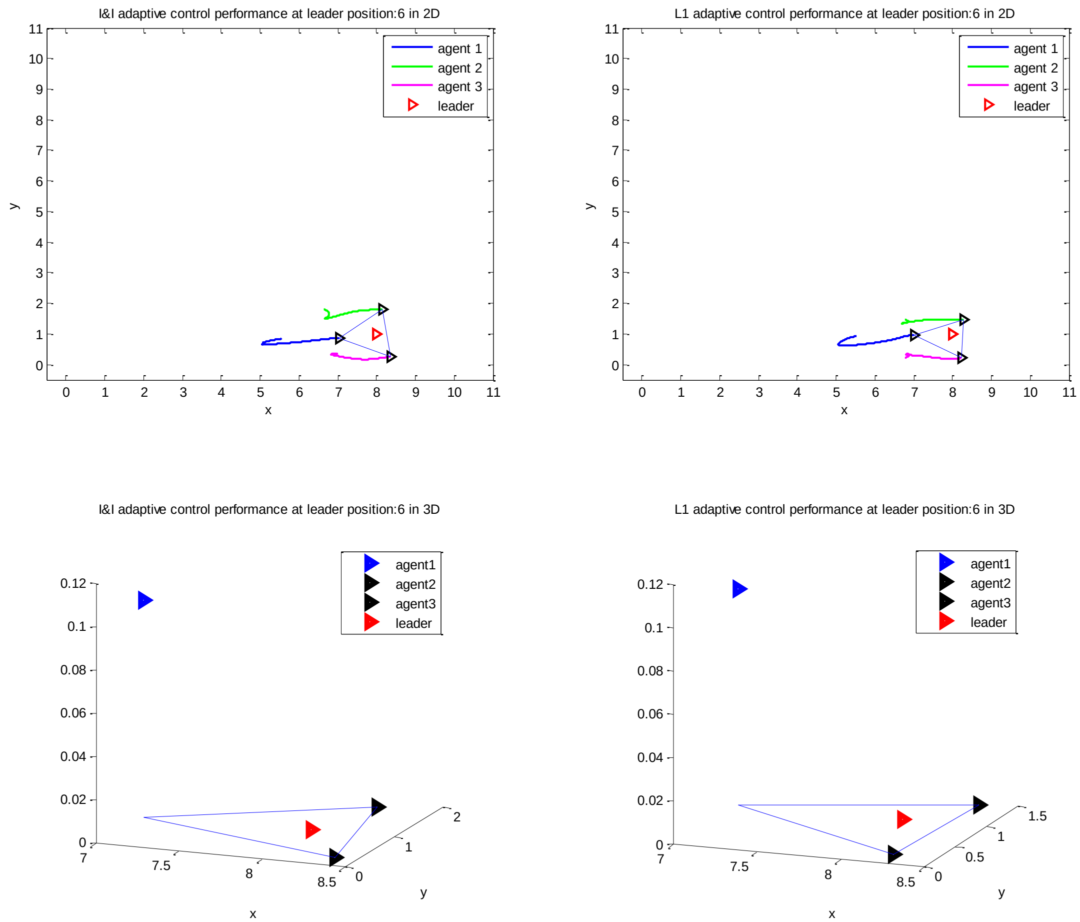

Figure 5.6 The group formation when the leader is at position $(\mathbf{8}, \mathbf{1})$.

Figure 5.6 shows the each agent move from position 5 to follow the leader at (8, 1). We can see the ability of I&I and L1 adaptive controllers to navigate each agent to track the desired formation.

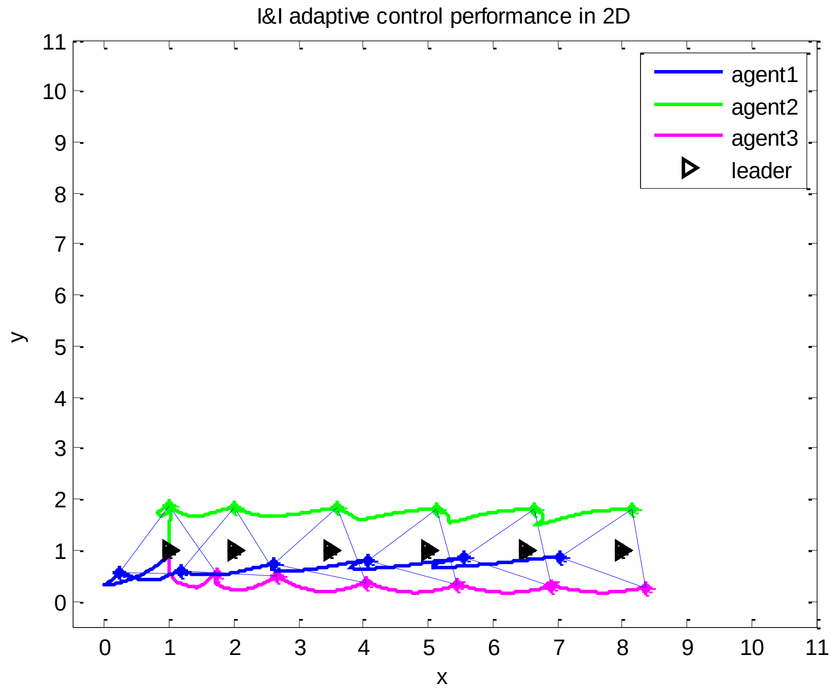

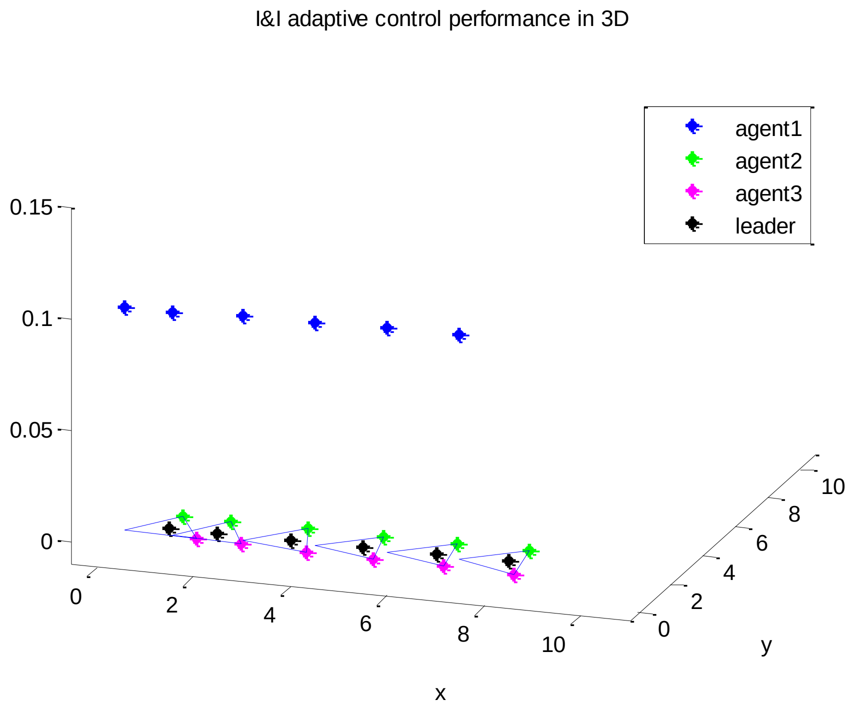

Figure 5.7 The group formation based I&I adaptive control on unknown maps.

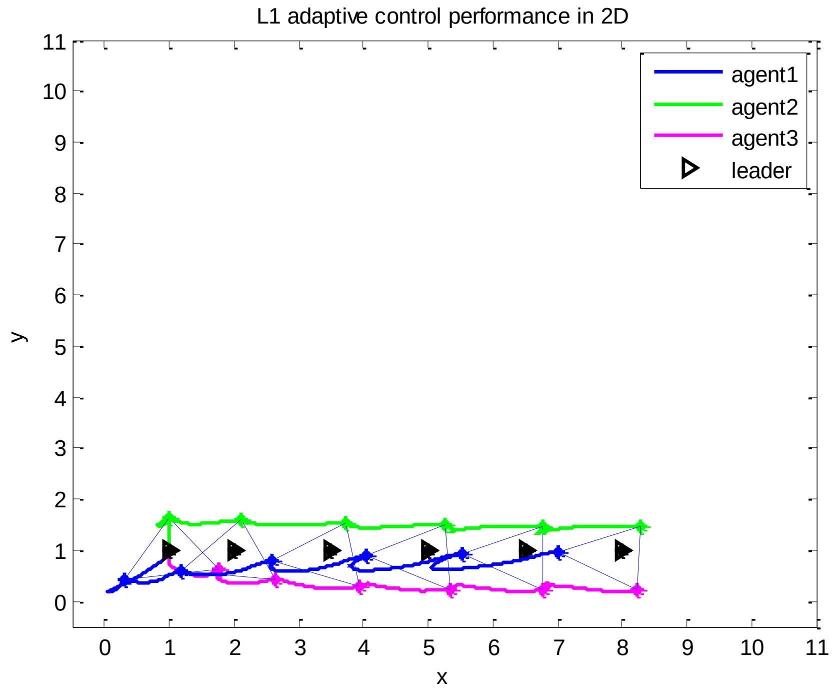

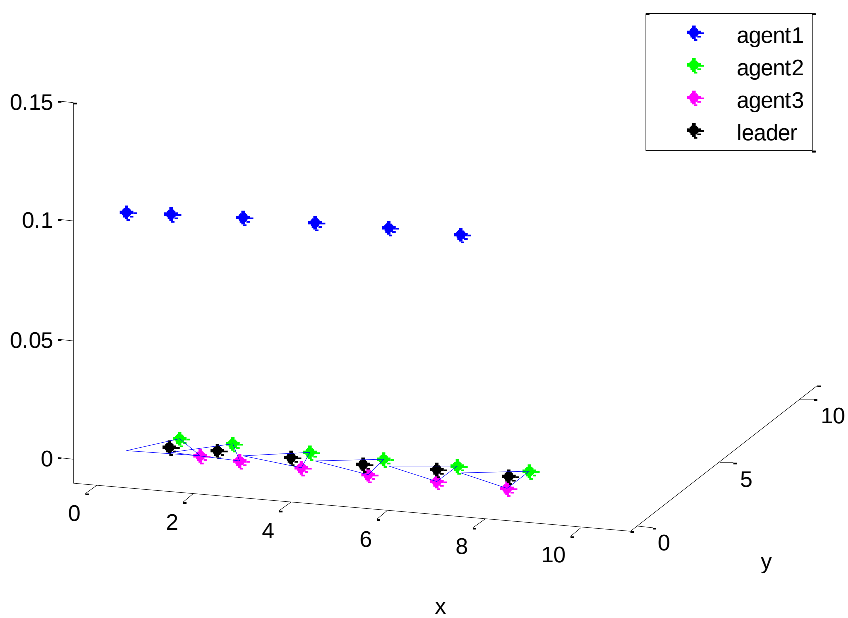

Figure 5.8 The group formation based L1 adaptive control on unknown maps.

Figure 5.7 and 5.8 show the comparison between I&I and L1 adaptive controllers performance along the whole navigation trajectory. Both controllers are able to navigate each agent to follow the particular position. We can see, the performance of I&I is better than L1 for adaptive cooperative control of heterogeneous systems in case 1. Table 5.1 shows the error position of formation control for case 1 in percentage (%).

Table 5.1. Error position of formation control for case 1

No	Leader Position	I&I		L1	
		EL (%)	ER (%)	EL (%)	ER (%)
1	(1, 1)	0.1592	0.1422	7.83	7.7431
2	(2, 1)	0.1973	0.0379	8.7804	8.7367
3	(3.5, 1)	0.2776	0.1735	9.5448	9.3812
4	(5, 1)	0.3514	0.3649	9.9102	9.6238
5	(6.5, 1)	0.4203	0.5437	10.1833	9.7934
6	(8, 1)	0.48	0.6994	10.3575	9.8835

Figure (5.9-5.18) show the comparison of I&I and L1 performance for adaptive cooperative control of heterogeneous systems in case 2. In this case, the leader moves about in x as well as y direction on unknown maps.

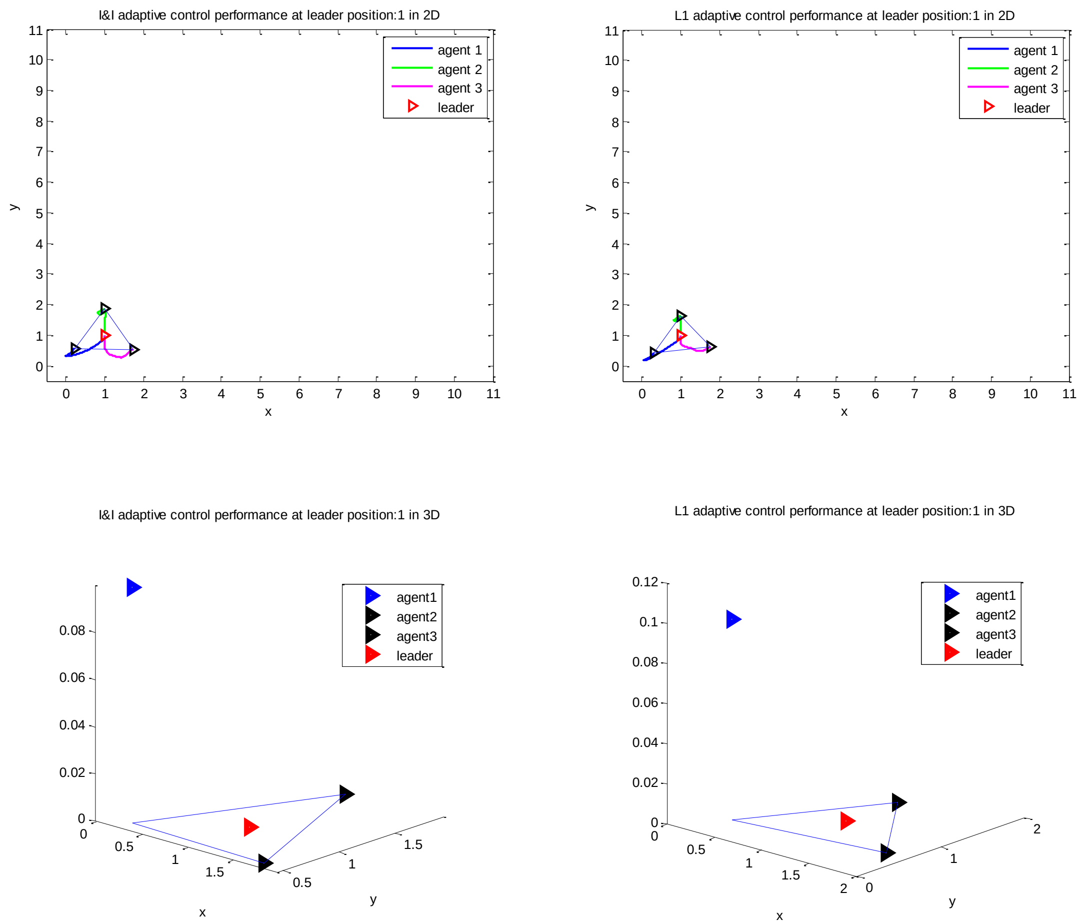

Figure 5.9 The group formation when the leader is at position $(\mathbf{1}, \mathbf{1})$.

Figure 5.9 shows the first agent move from (1.02, 1), second agent from (1, 1.08) and third agent from (1, 0.99) respectively to follow the leader at (1, 1). We can see the ability of I&I and L1 adaptive controllers to navigate each agent to track the desired formation.

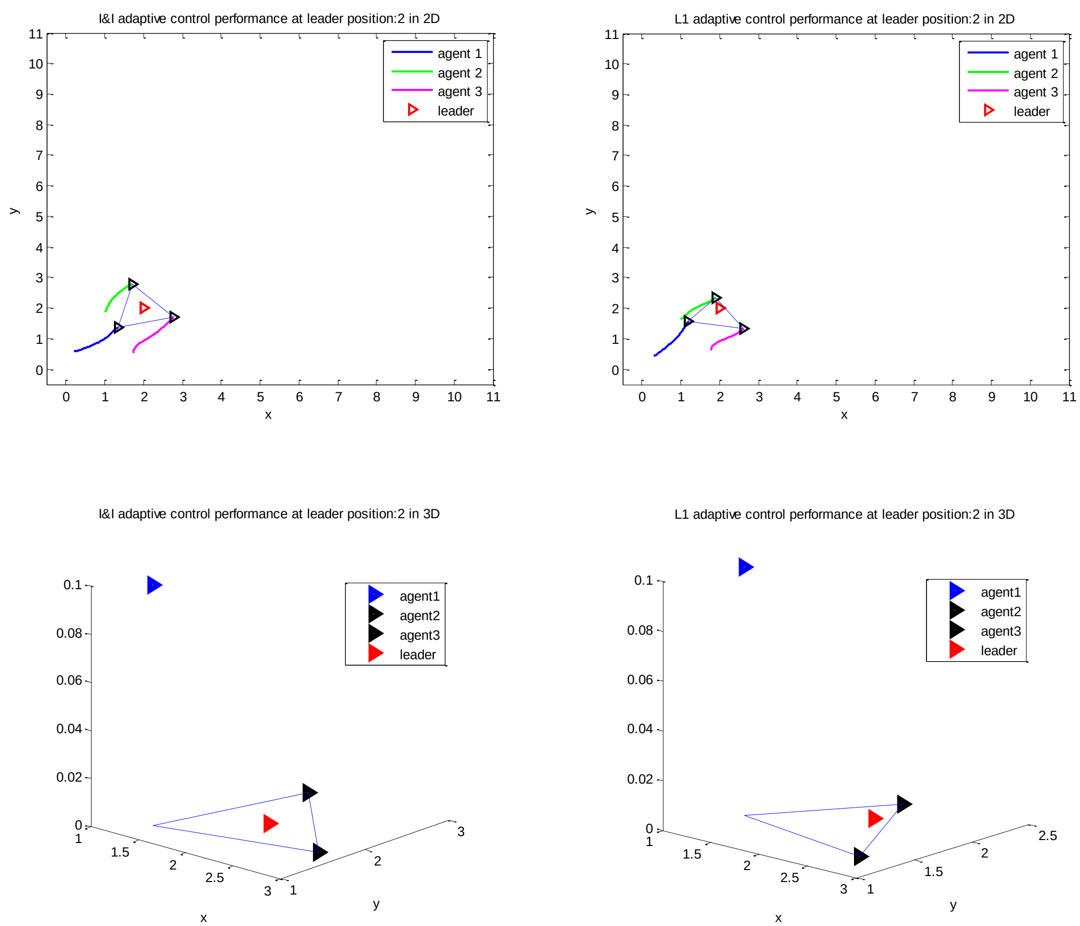

Figure 5.10 The group formation when the leader is at position $(\mathbf{2}, \mathbf{2})$.

Figure 5.10 shows the each agent move from position 1 to follow the leader at (2, 2). We can see the ability of I&I and L1 adaptive controllers to navigate each agent to track the desired formation.

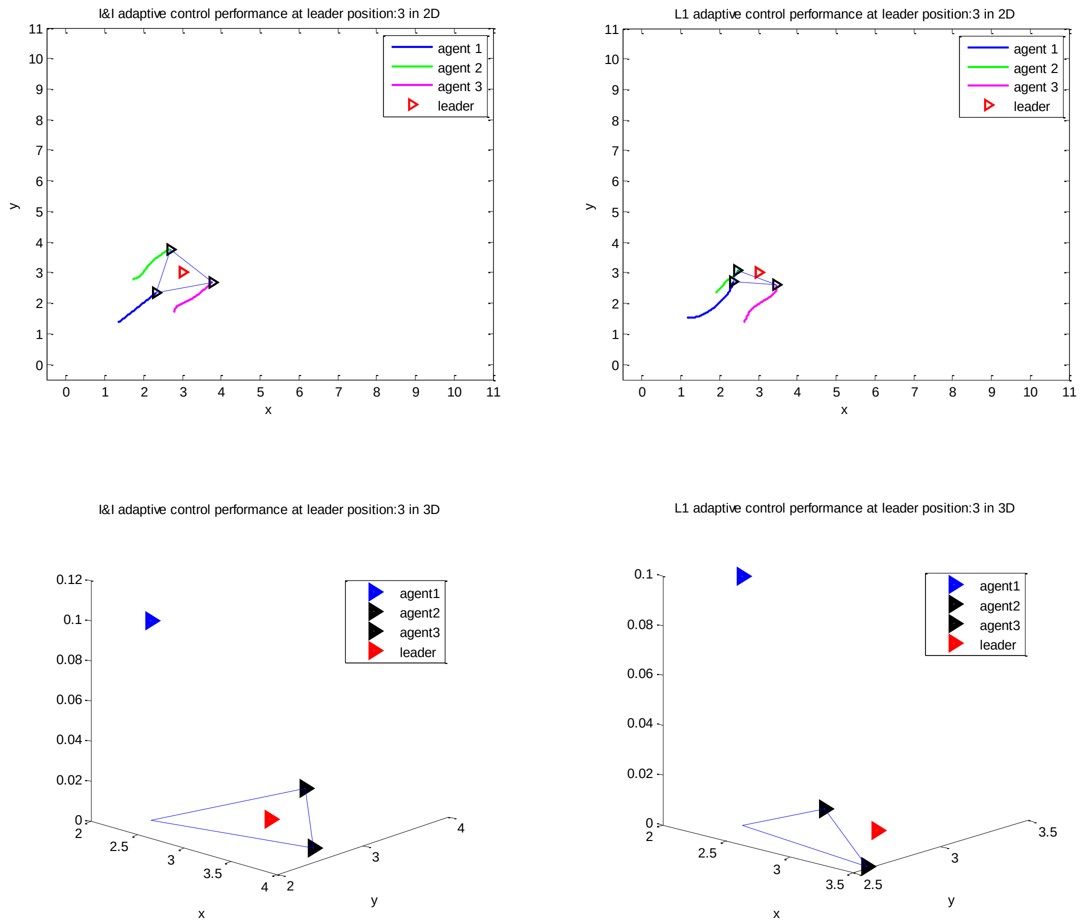

Figure 5.11 The group formation when the leader is at position $(\mathbf{3}, \mathbf{3})$.

Figure 5.11 shows the each agent move from position 2 to follow the leader at (3, 3). We can see the I&I approach is able to navigate each agent to follow the desired formation and L1 failed to track the desired formation.

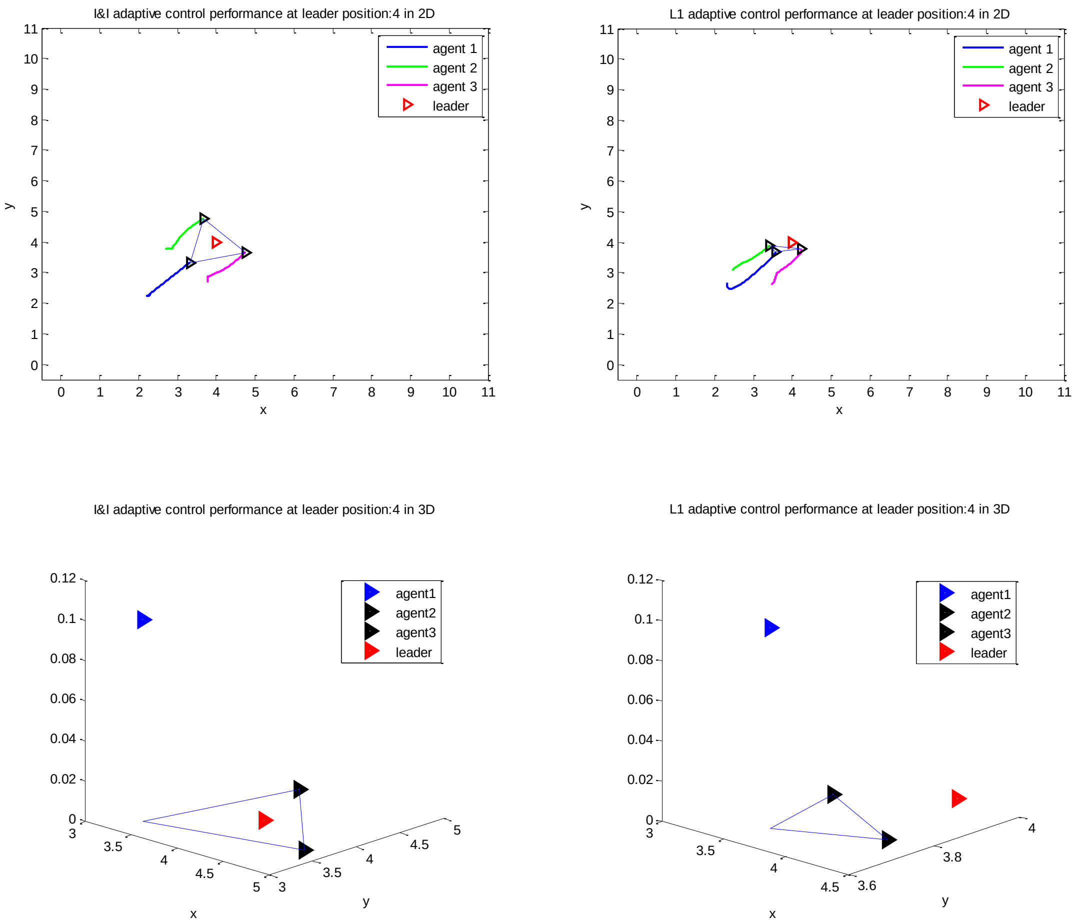

Figure 5.12 The group formation when the leader is at position$(\mathbf{4}, \mathbf{4})$.

Figure 5.12 shows the each agent move from position 3 to follow the leader at (4, 4). We can see the I&I approach is able to navigate each agent to follow the desired formation and L1 failed to track the desired formation.

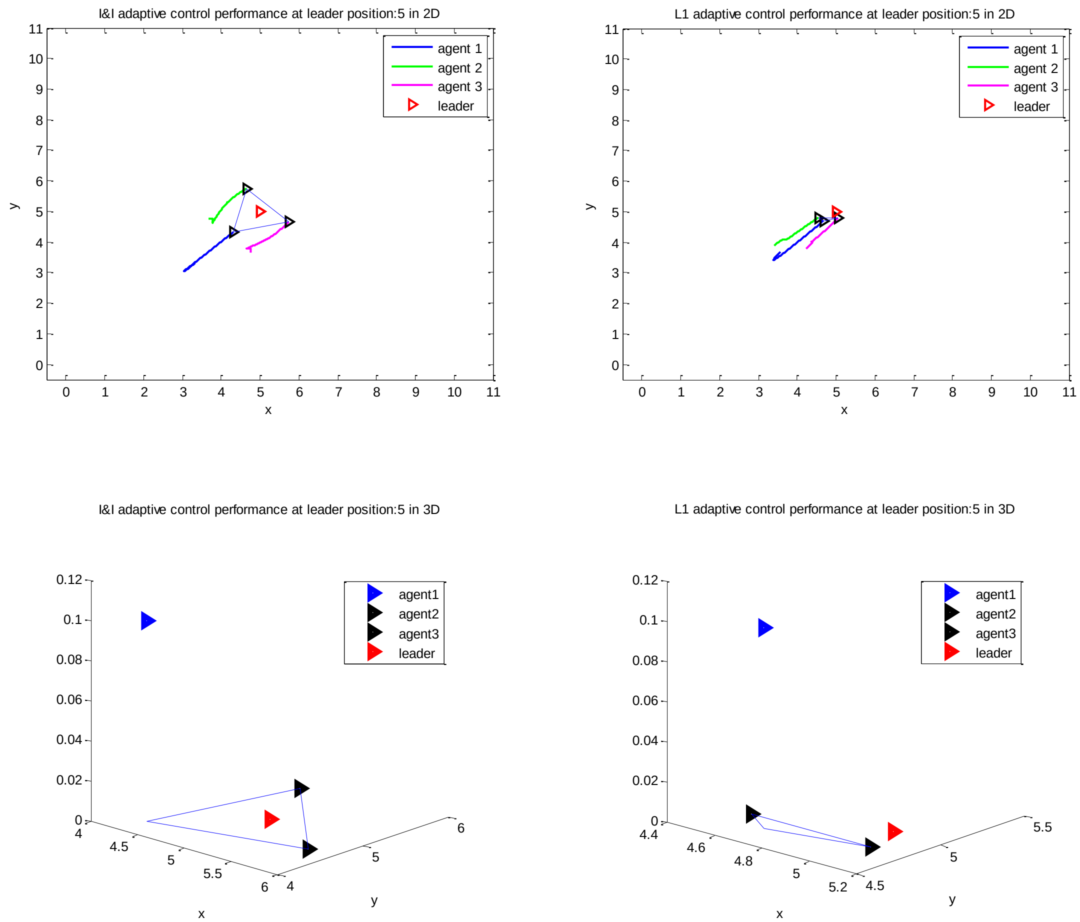

Figure 5.13 The group formation when the leader is at position $(\mathbf{5}, \mathbf{5})$

Figure 5.13 shows the each agent move from position 4 to follow the leader at (5, 5). We can see the I&I approach is able to navigate each agent to follow the desired formation and L1 failed to track the desired formation.

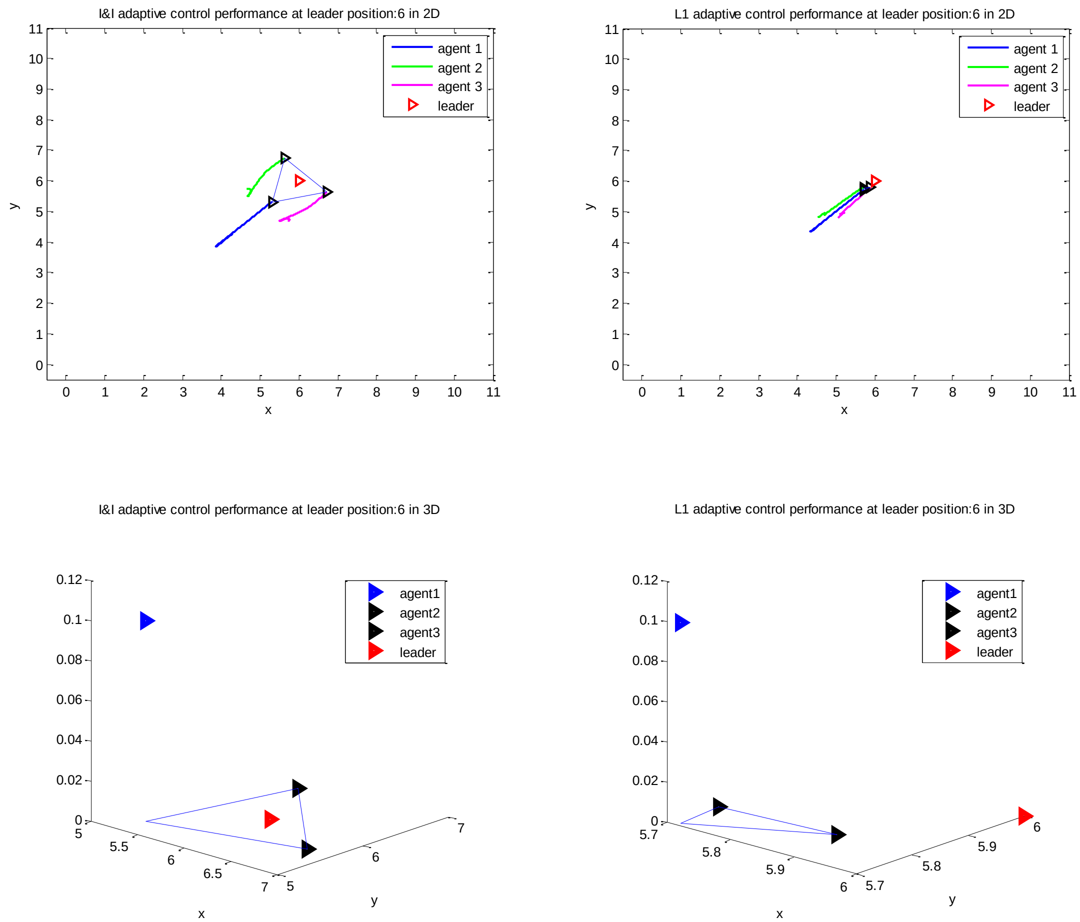

Figure 5.14 The group formation when the leader is at position $(\mathbf{6}, \mathbf{6})$.

Figure 5.14 shows the each agent move from position 5 to follow the leader at (6, 6). We can see the I&I approach is able to navigate each agent to follow the desired formation and L1 failed to track the desired formation.

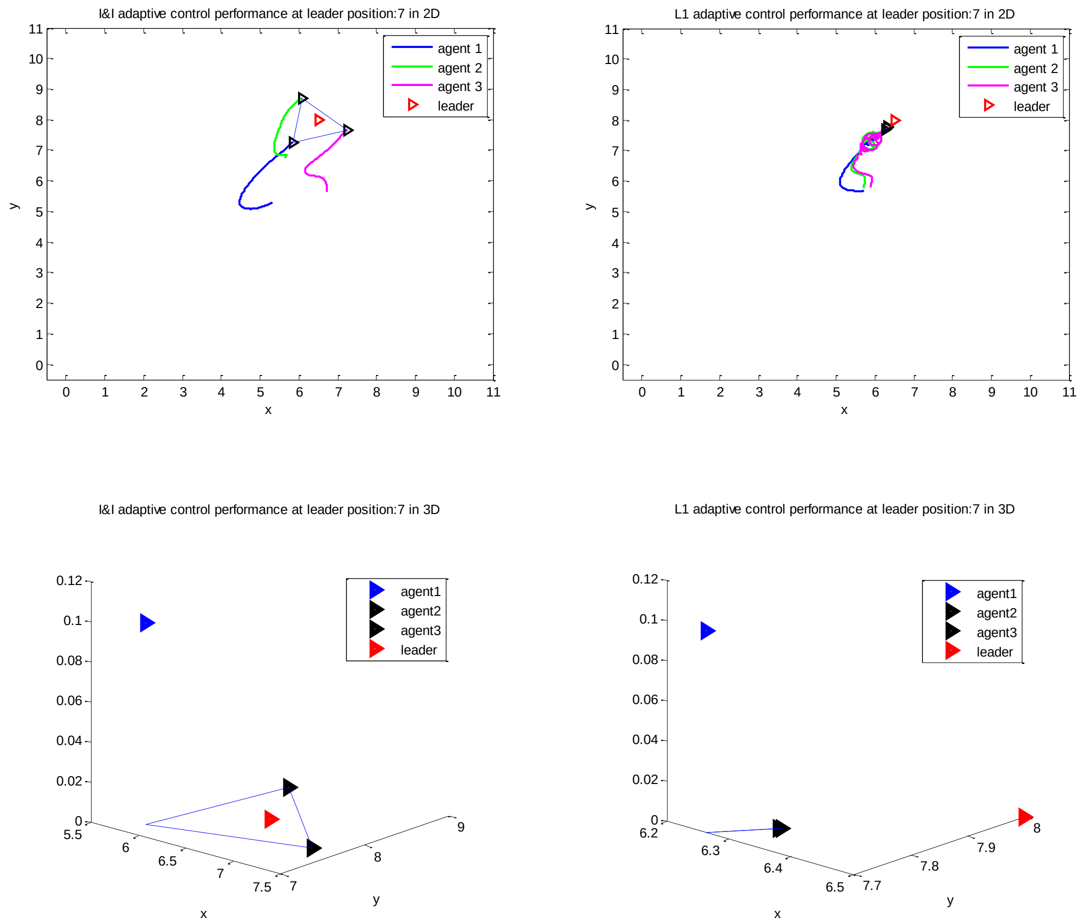

Figure 5.15 The group formation when the leader is at position $(\mathbf{6.5, 8})$.

Figure 5.15 shows the each agent move from position 6 to follow the leader at (6.5, 8). We can see the I&I approach is able to navigate each agent to follow the desired formation and L1 failed to track the desired formation.

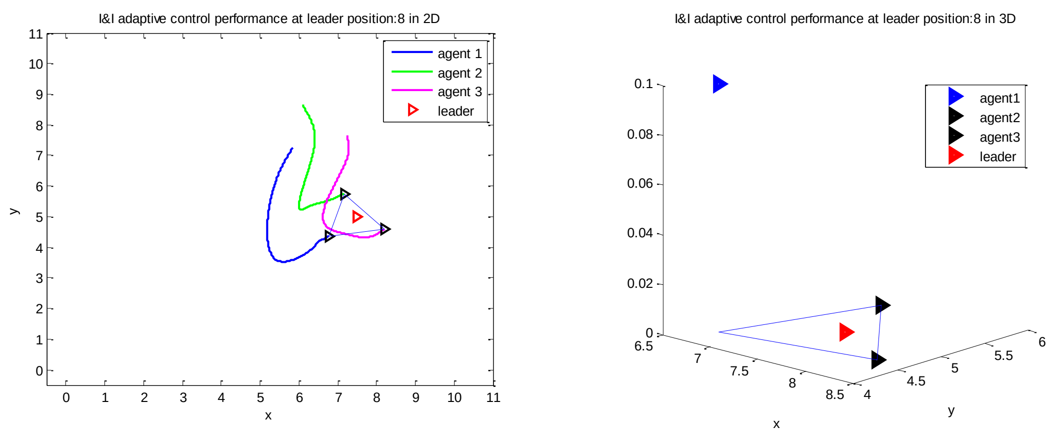

Figure 5.16 The group formation when the leader is at position $(\mathbf{7.5}, \mathbf{5})$

Figure 5.16 shows the each agent move from position 7 to follow the leader at (7.5, 5). We can see the I&I approach is able to navigate each agent to follow the desired formation. Matlab failed to simulate formation control based on L1 in this position.

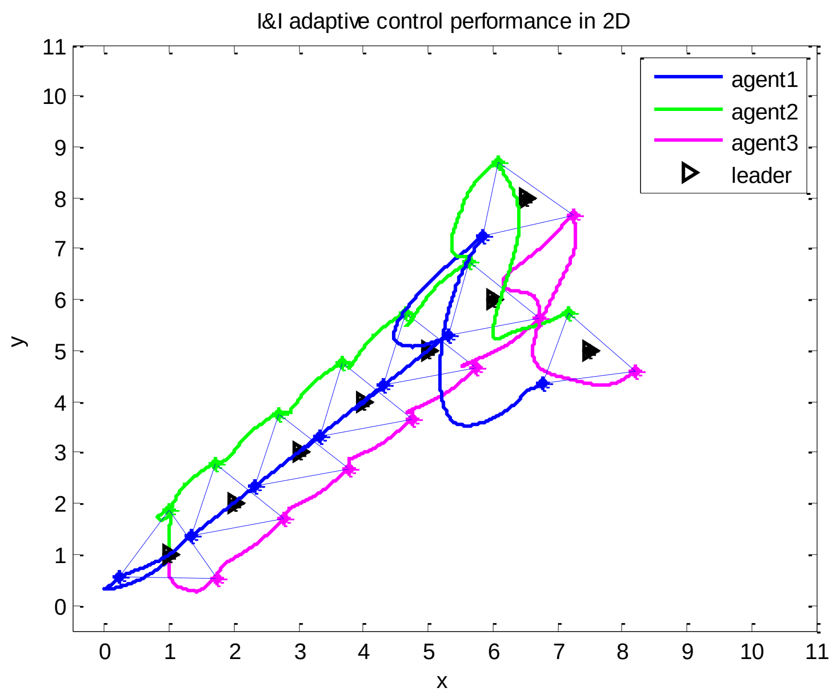

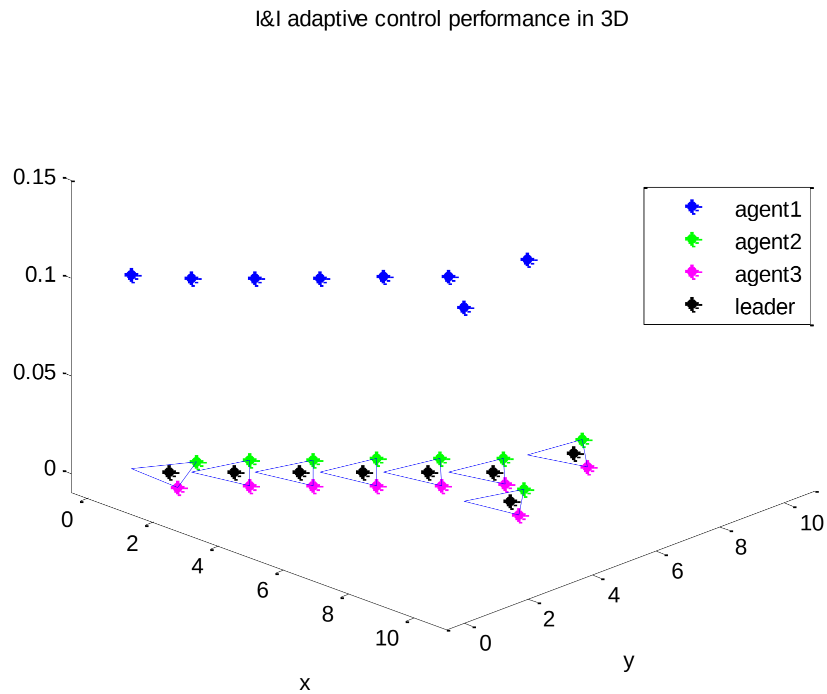

Figure 5.17 The group formation based I&I adaptive control on unknown maps

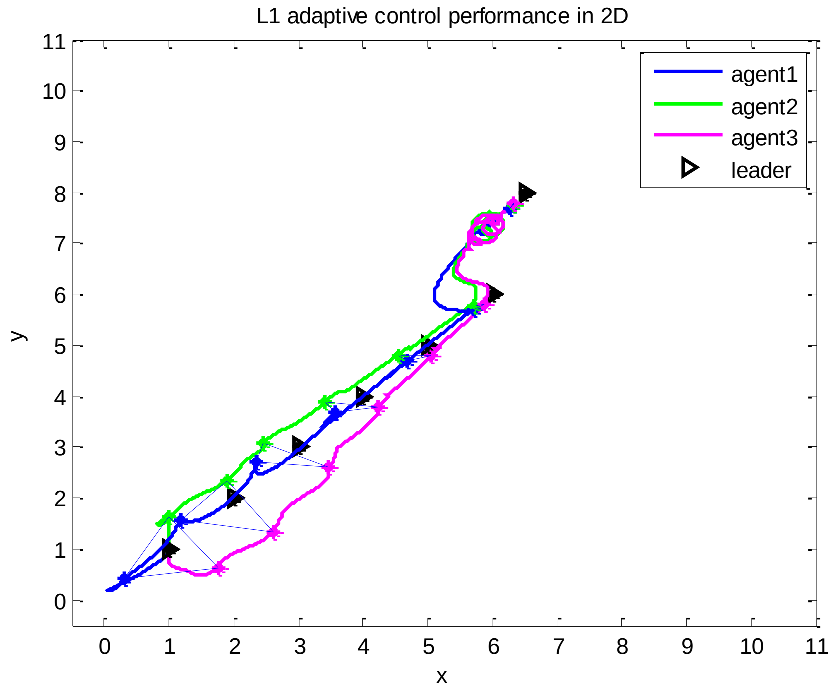

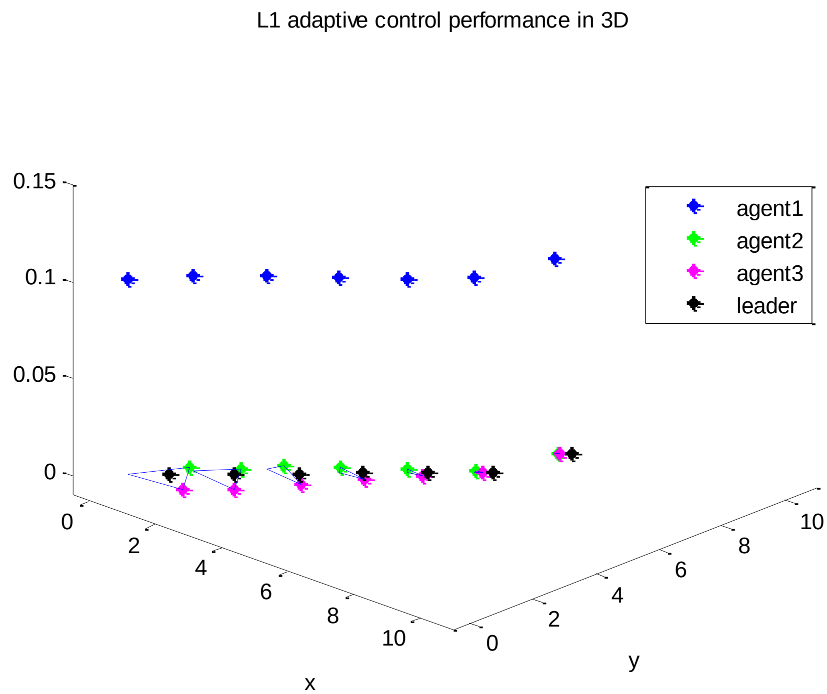

Figure 5.18 The group formation based L1 adaptive control on unknown maps

Figure 5.17 and 5.18 give the comparison between I&I and L1 adaptive controllers performance along the whole navigation trajectory. We can see, the ability of I&I is better than L1 for adaptive cooperative control of heterogeneous systems in case 2. Table 5.2 shows the error formation control for case 2 in percentage (%).

Table 5.2. Error position of formation control for case 2

No	Leader Position	I&I		L1	
		EL (%)	ER (%)	EL (%)	ER (%)
1	(1, 1)	0.1592	0.1422	7.83	7.7431
2	(2, 2)	0.2342	0.0603	16.8974	15.7989
3	(3, 3)	0.3055	0.2463	41.5762	28.0381
4	(4, 4)	0.3781	0.4342	60.9157	43.5121
5	(5, 5)	0.4402	0.5979	76.3222	55.4936
6	(6, 6)	0.4934	0.738	90.1706	61.2744
7	(6.5, 8)	0.5468	0.8778	95.9638	62.7246
8	(7.5, 5)	0.4947	0.7479	Matlab error	

5.3 Adaptive Cooperative Control of Nonholonomic Mobile Robots

We present the performance of adaptive cooperative control based on neuro I&I for multi nonholonomic mobile robots and compare its performance with adaptive cooperative control based on neuro I&I, I&I and L1. The desired position respect to x-axis and y-ordinate are selected as set point system respectively. In simulation, the result obtained that the cooperative control based on neuro I&I adaptive control is able to follow the desired formation.

Figure (5.19-5.35) show the comparison of neuro I&I, I&I and L1 for adaptive cooperative control of homogeneous systems. We apply the control strategies for 3 nonholonomic mobile robots moving together in group formation on unknown fleet maps.

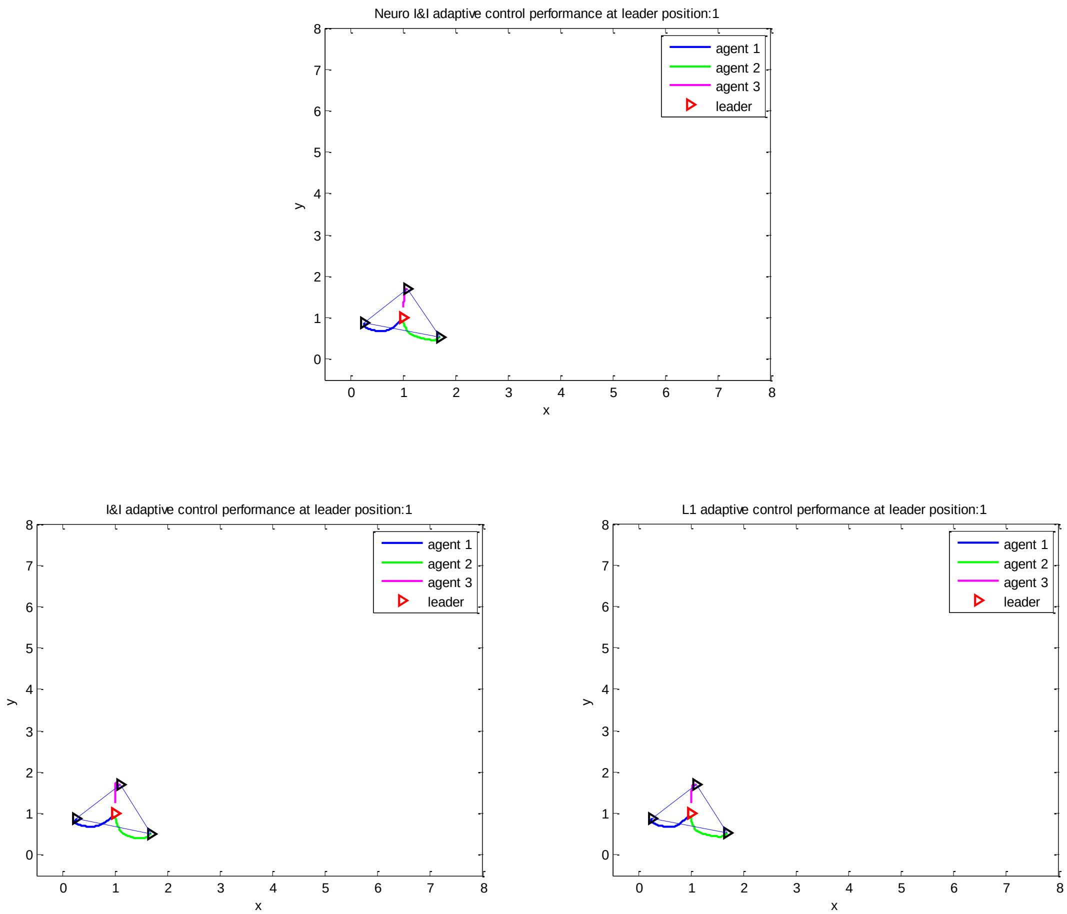

Figure 5.19 The group formation when the leader is at position $(\mathbf{1}, \mathbf{1})$.

Figure 5.19 shows the first agent move from (0.95, 0.95), second agent from (1, 0.95) and third agent from (1, 1.25) respectively to follow the leader at (1, 1). We can see the ability of neuro I&I, I&I and L1 adaptive controllers to navigate each agent to track the desired formation.

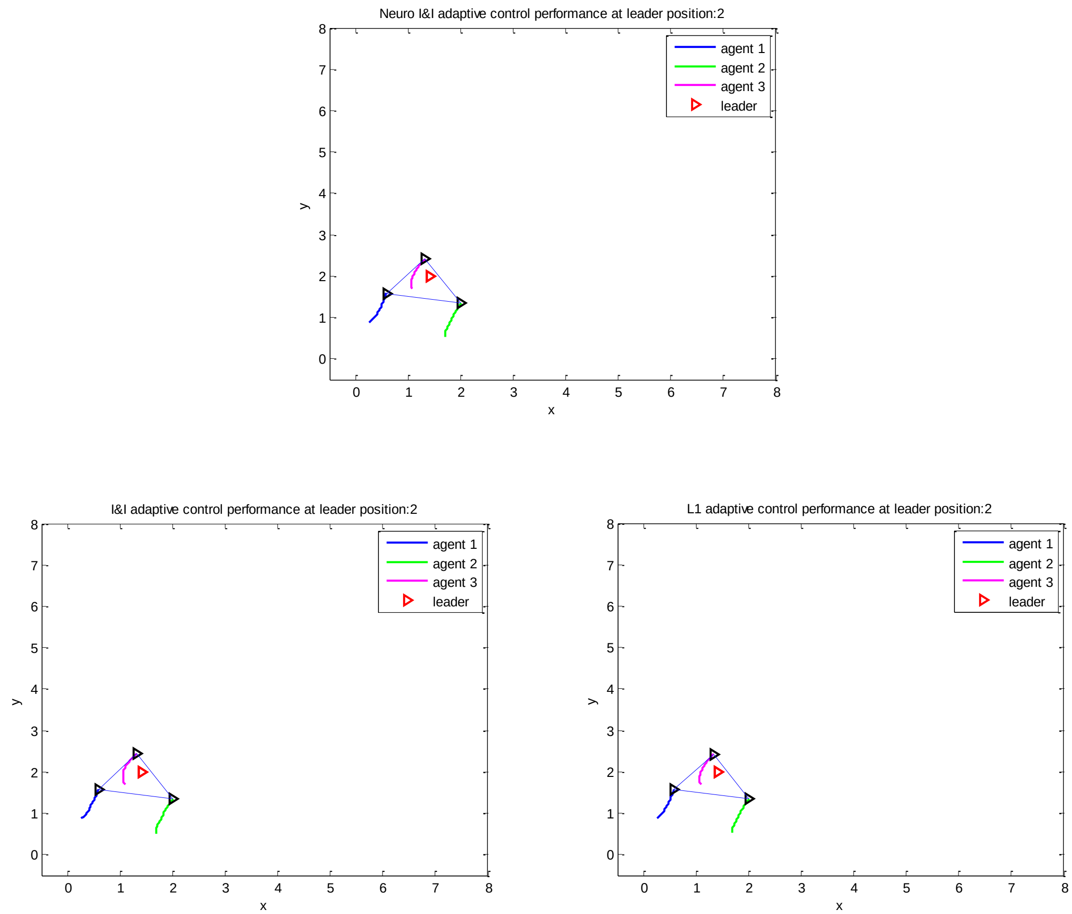

Figure 5.20 The group formation when the leader is at position $(\mathbf{1.4, 2})$.

Figure 5.20 shows the each agent move from position 1 to follow the leader at (1.4, 2). We can see the ability of neuro I&I, I&I and L1 adaptive controllers to navigate each agent to track the desired formation.

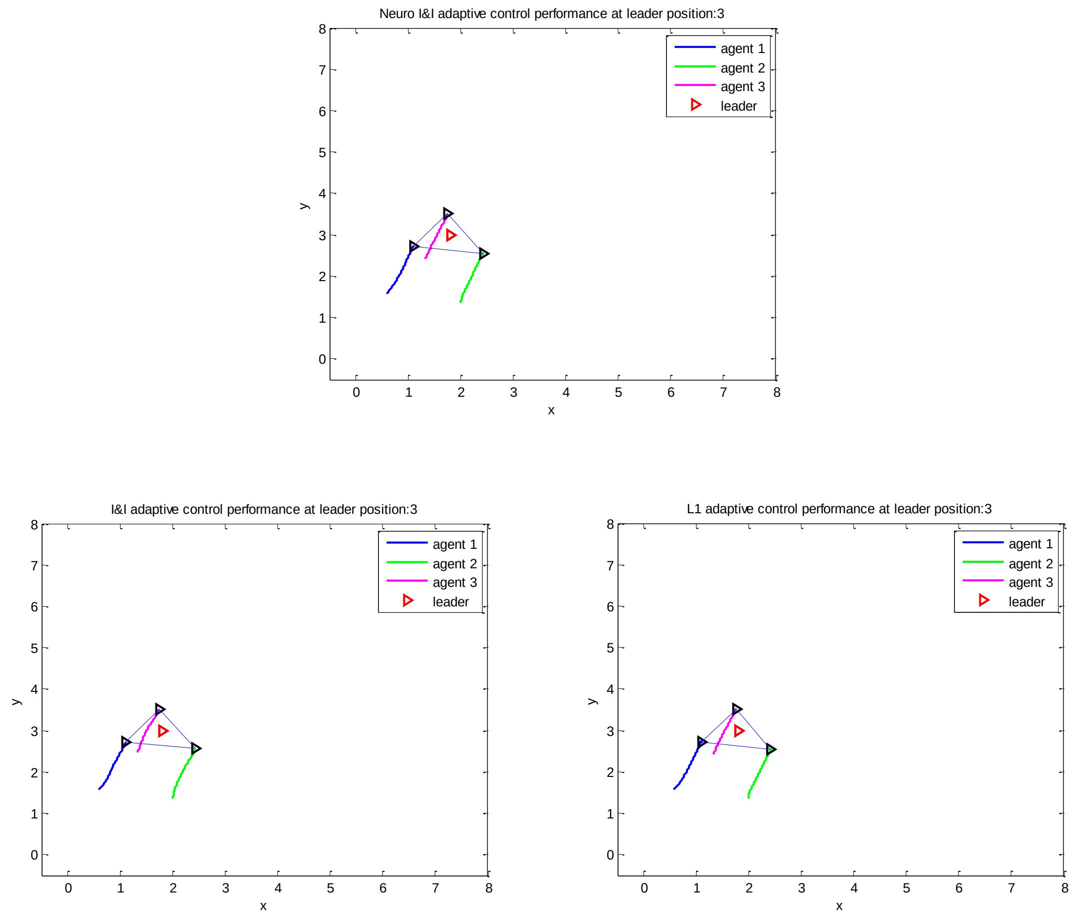

Figure 5.21 The group formation when the leader is at position $(\mathbf{1.8, 3})$

Figure 5.21 shows the each agent move from position 2 to follow the leader at (1.8, 3). We can see the ability of neuro I&I, I&I and L1 adaptive controllers to navigate each agent to track the desired formation.

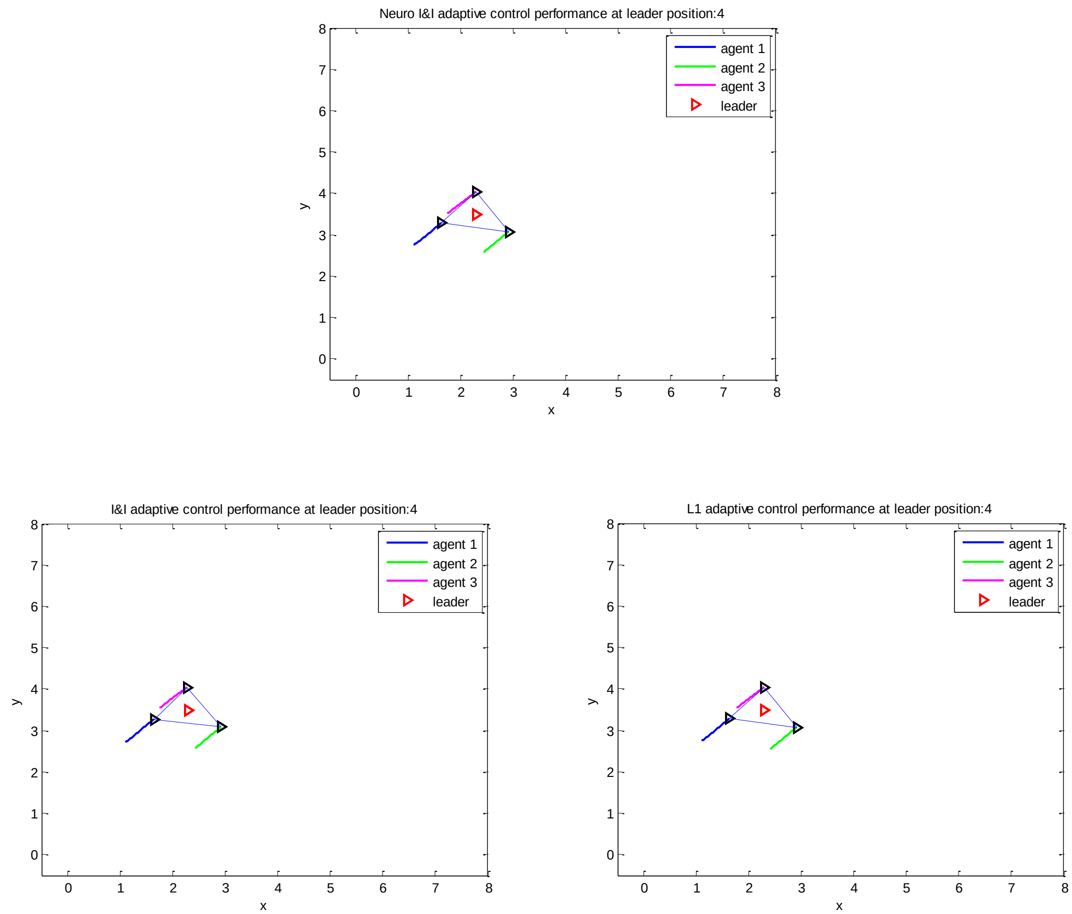

Figure 5.22 The group formation when the leader is at position $(\mathbf{2.3}, \mathbf{3.5})$

Figure 5.22 shows the each agent move from position 3 to follow the leader at (2.3, 3.5). We can see the ability of neuro I&I, I&I and L1adaptive controllers to navigate each agent to track the desired formation.

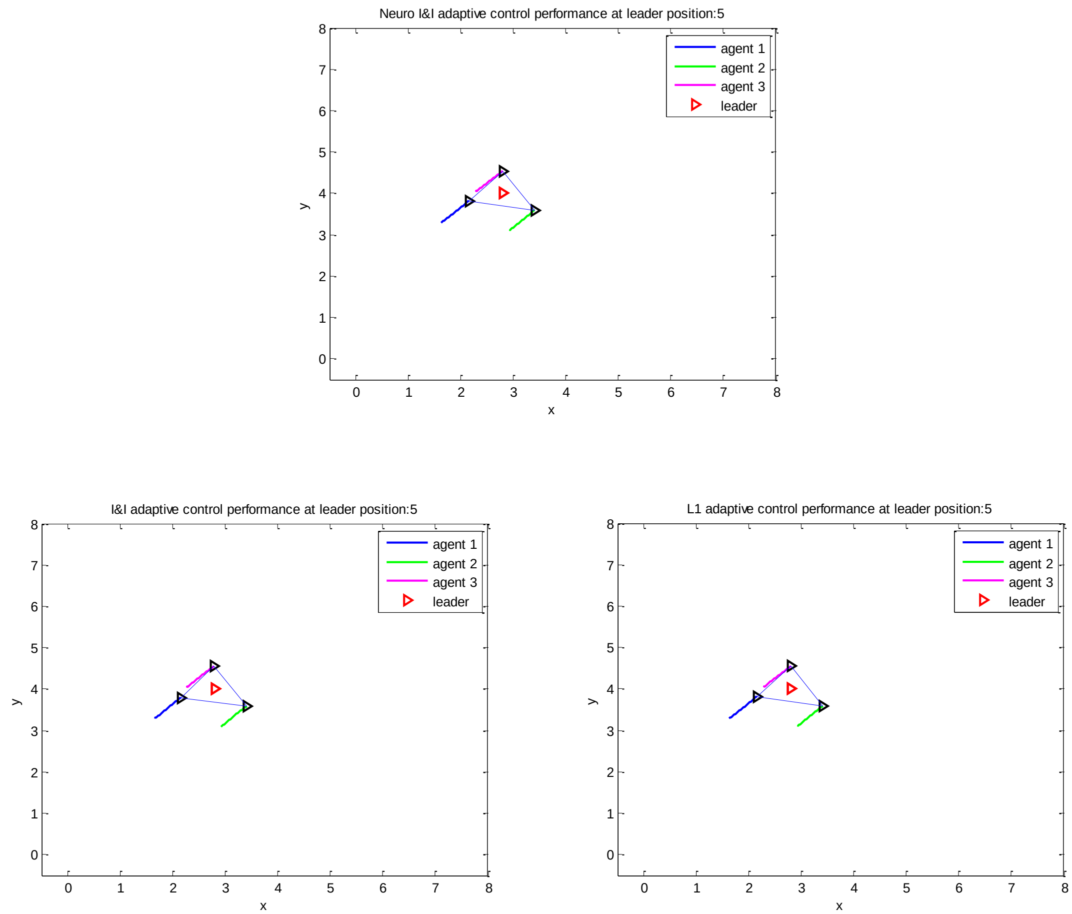

Figure 5.23 The group formation when the leader is at position $(\mathbf{2.8, 4})$

Figure 5.23 shows the each agent move from position 4 to follow the leader at (2.8, 4). We can see the ability of neuro I&I, I&I and L1 adaptive controllers to navigate each agent to track the desired formation.

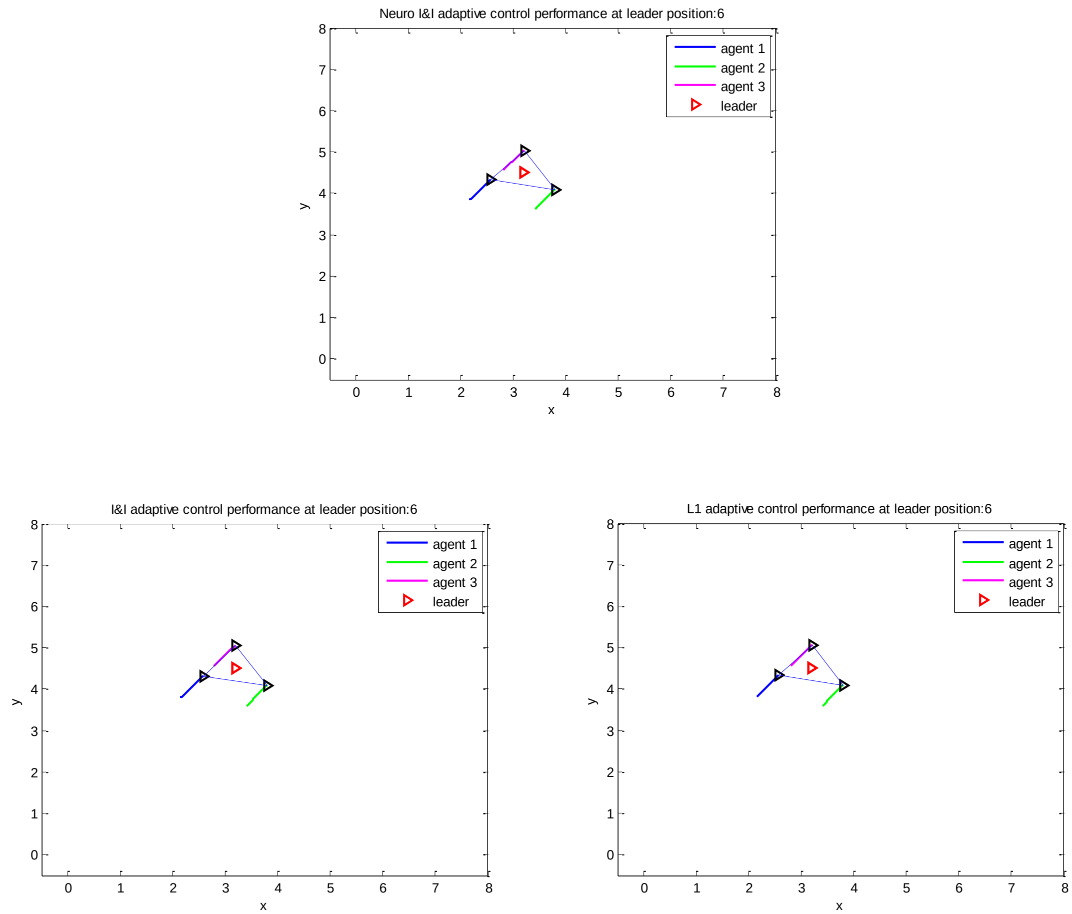

Figure 5.24 The group formation when the leader is position $(\mathbf{3.2}, \mathbf{4.5})$.

Figure 5.24 shows the each agent move from position 5 to follow the leader at (3.2, 4.5). We can see the ability of neuro I&I, I&I and L1 adaptive controllers to navigate each agent to track the desired formation.

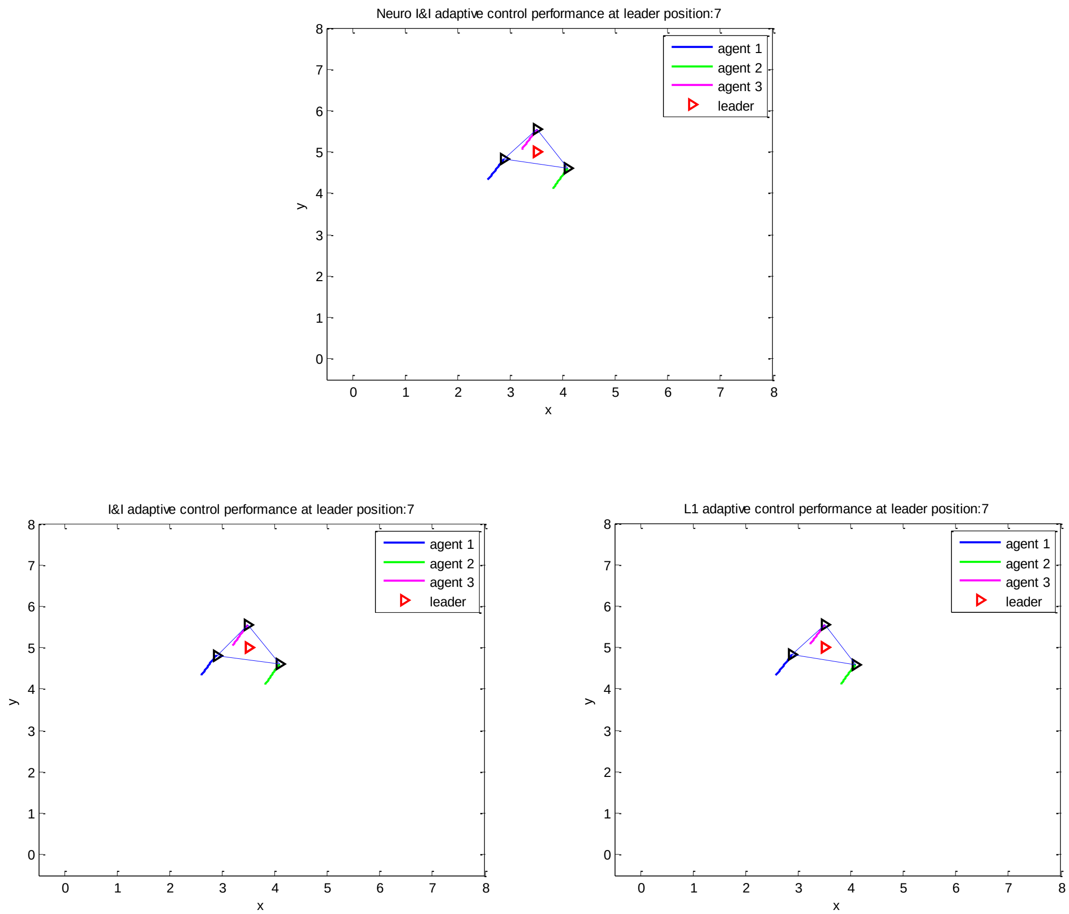

Figure 5.25 The group formation when the leader is at position $(\mathbf{3.5, 5})$.

Figure 5.25 shows the each agent move from position 6 to follow the leader at (3.5, 5). We can see the ability of neuro I&I, I&I and L1 adaptive controllers to navigate each agent to track the desired formation.

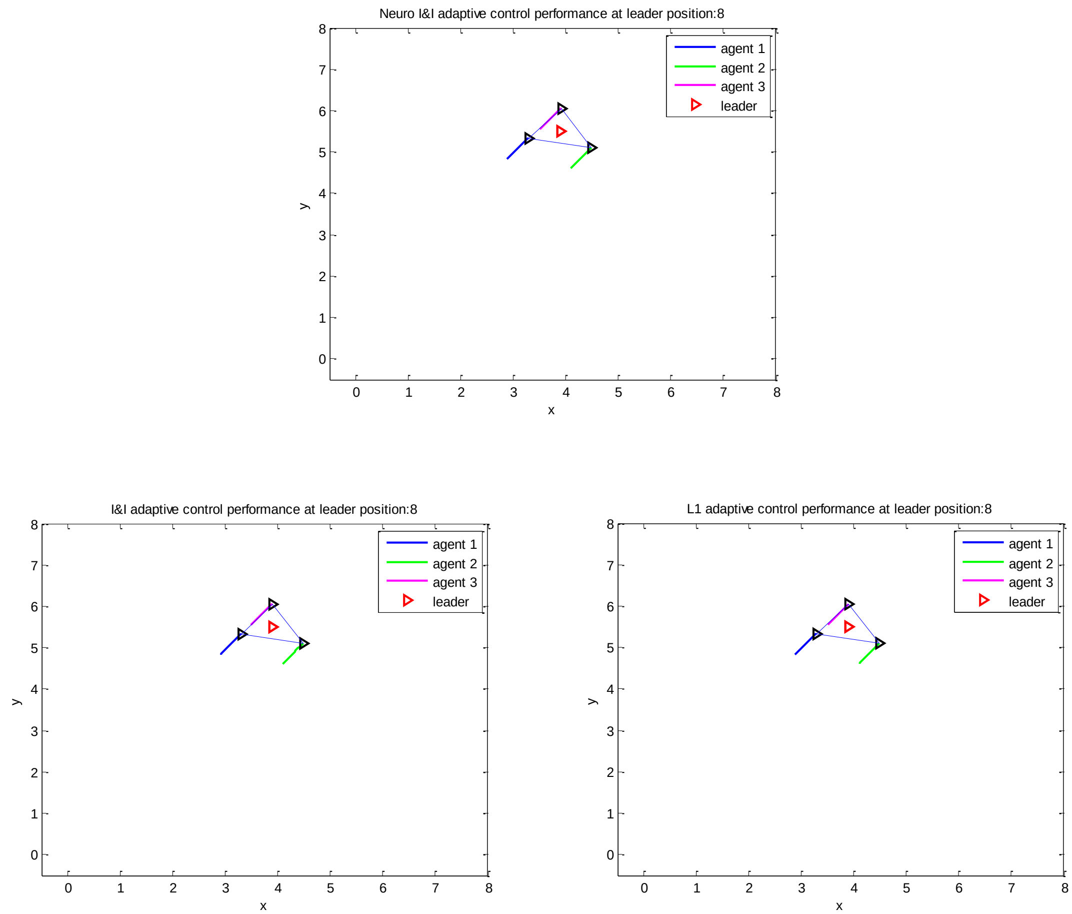

Figure 5.26 The group formation when the leader is at position $(\mathbf{3.9, 5.5})$.

Figure 5.26 shows the each agent move from position 7 to follow the leader at (3.9, 5.5). We can see the ability of neuro I&I, I&I and L1 adaptive controllers to navigate each agent to track the desired formation.

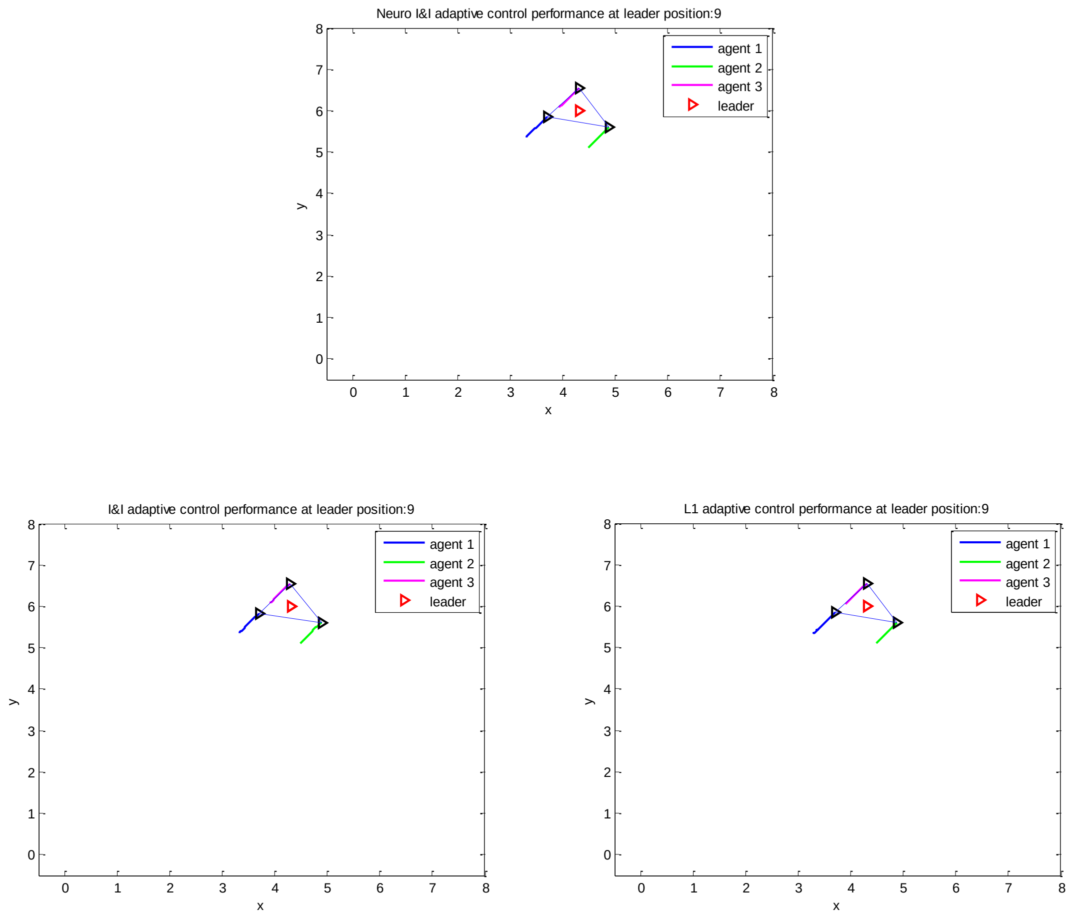

Figure 5.27 The group formation when the leader is at position $(\mathbf{4.3}, \mathbf{6})$.

Figure 5.27 shows the each agent move from position 8 to follow the leader at (4.3, 6). We can see the ability of neuro I&I, I&I and L1 adaptive controllers to navigate each agent to track the desired formation.

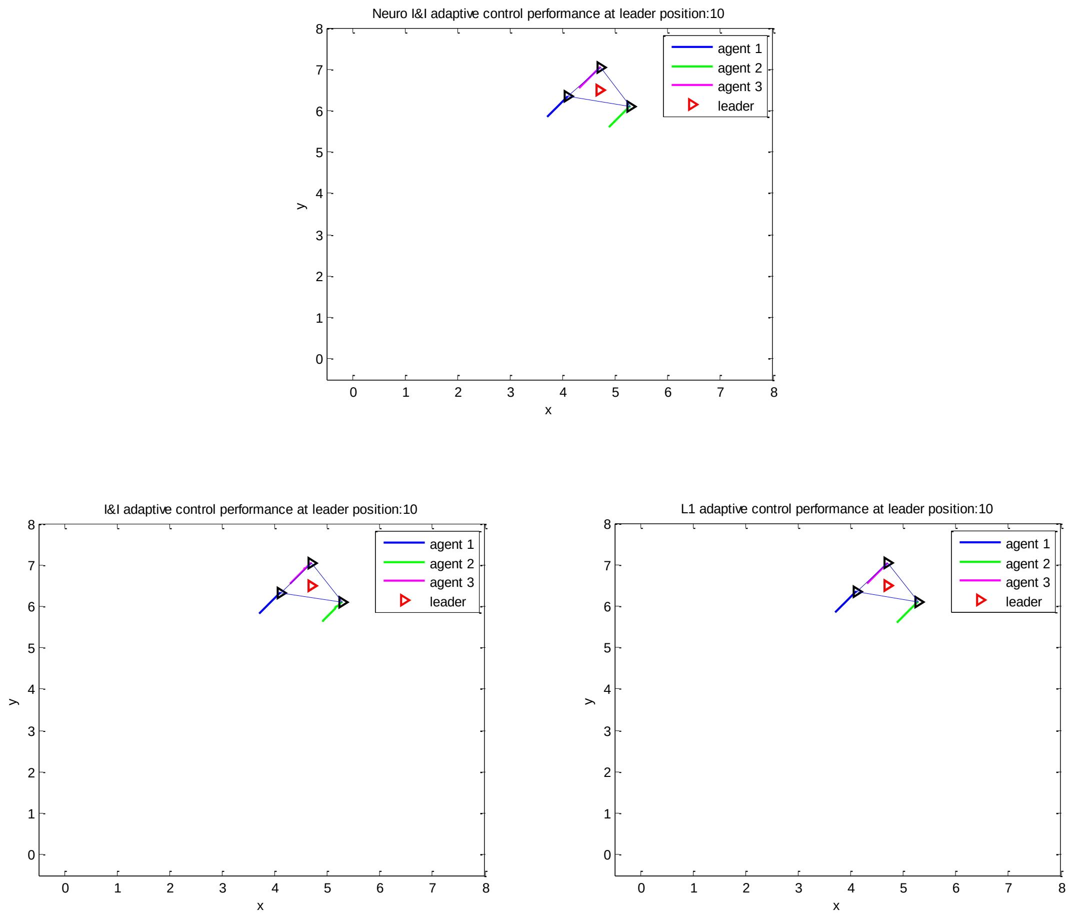

Figure 5.28 The group formation when the leader is at position $(\mathbf{4.7, 6.5})$.

Figure 5.28 shows the each agent move from position 9 to follow the leader at (4.7, 6.5). We can see the ability of neuro I&I, I&I and L1 adaptive controllers to navigate each agent to track the desired formation.

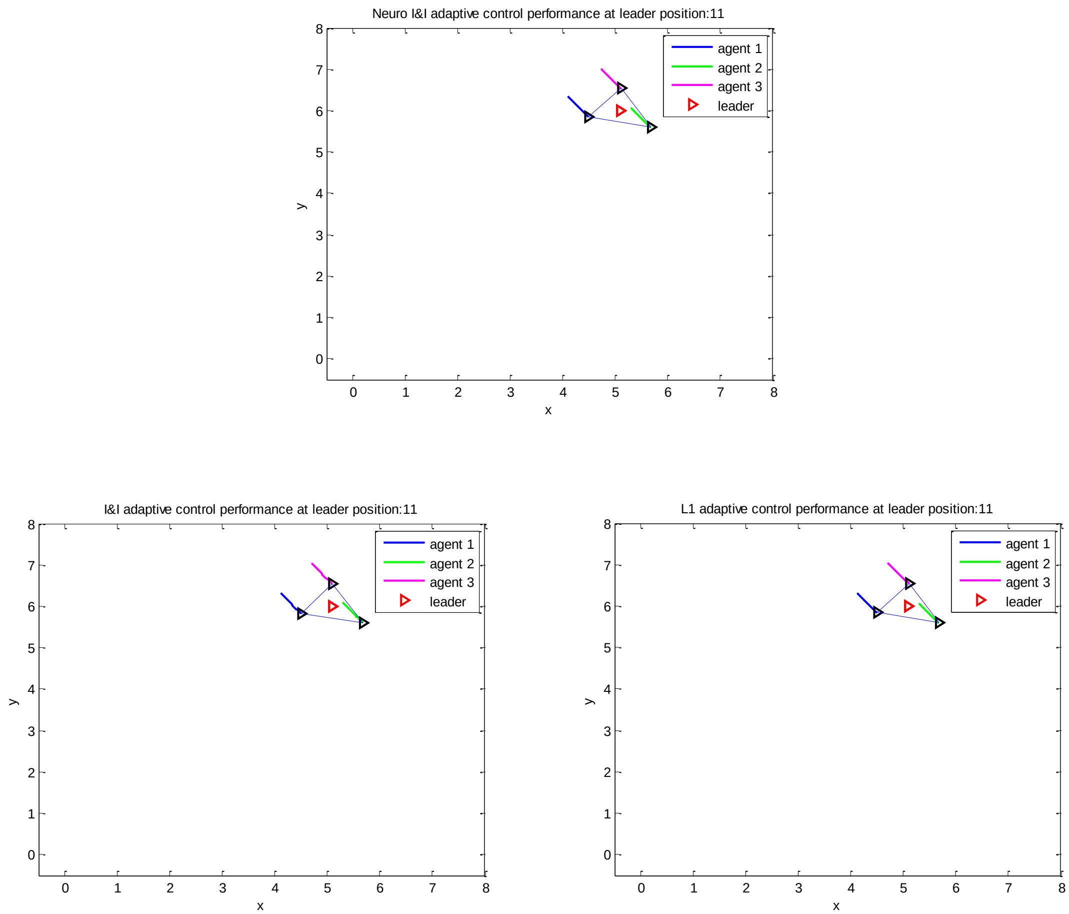

Figure 5.29 The group formation when the leader is at position $(\mathbf{5.1}, \mathbf{6})$.

Figure 5.29 shows the each agent move from position 10 to follow the leader at (5.1, 6). We can see the ability of neuro I&I, I&I and L1 adaptive controllers to navigate each agent to track the desired formation.

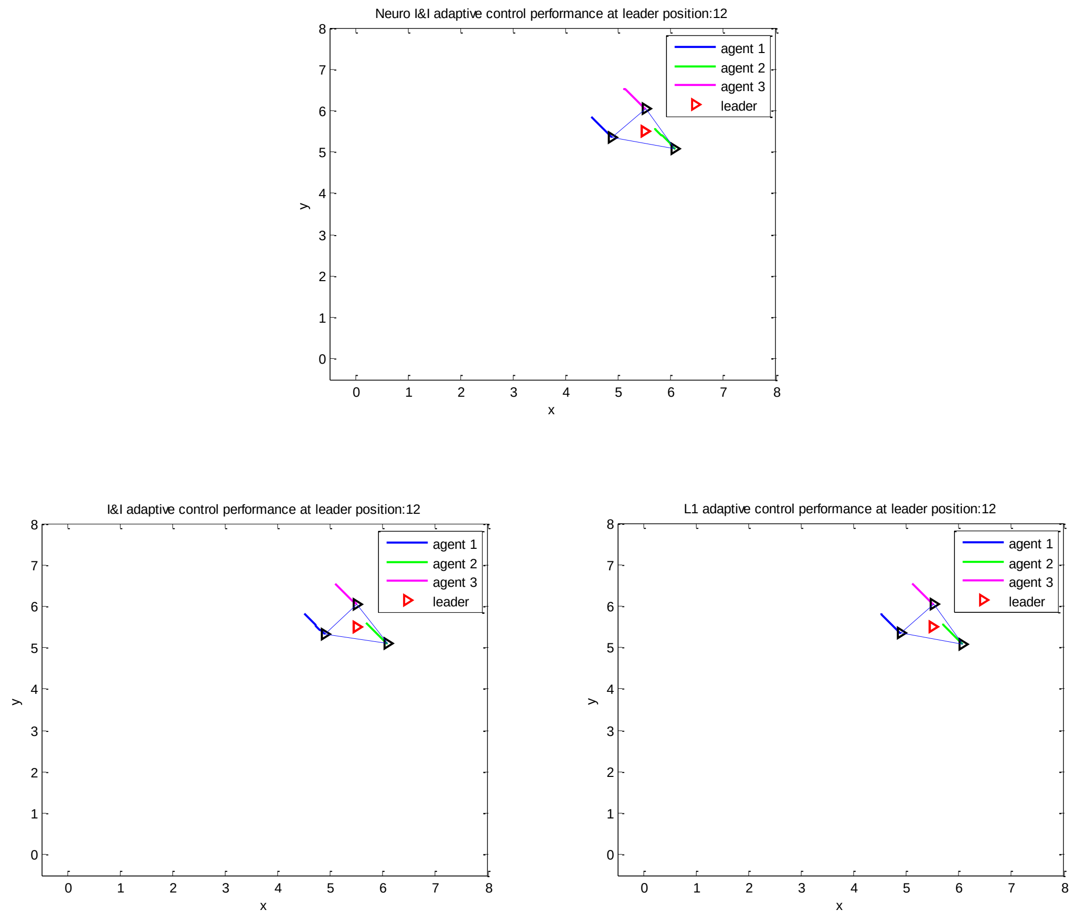

Figure 5.30 The group formation when the leader is at position $(\mathbf{5.5}, \mathbf{5.5})$.

Figure 5.30 shows the each agent move from position 11 to follow the leader at (5.5, 5.5). We can see the ability of neuro I&I, I&I and L1 adaptive controllers to navigate each agent to track the desired formation.

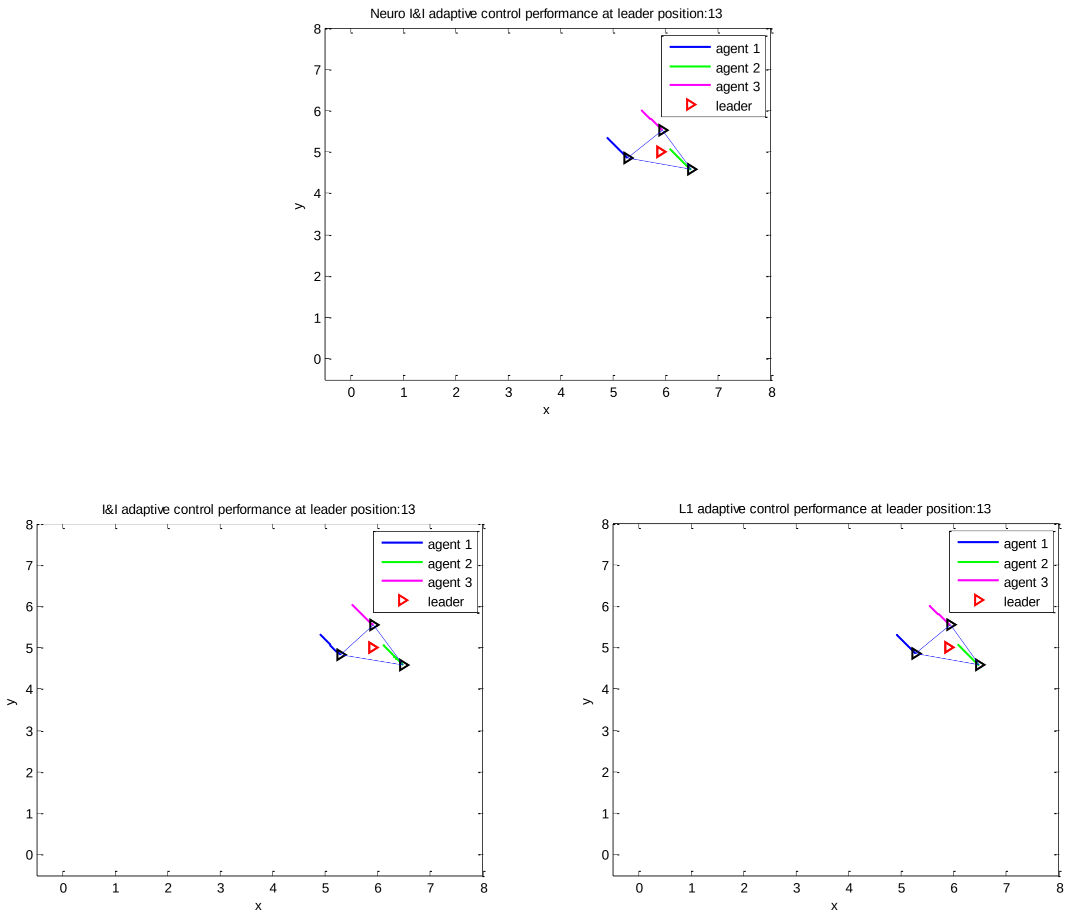

Figure 5.31 The group formation when the leader is at position $(\mathbf{5.9, 5})$.

Figure 5.31 shows the each agent move from position 12 to follow the leader at (5.9, 5). We can see the ability of neuro I&I, I&I and L1 adaptive controllers to navigate each agent to track the desired formation.

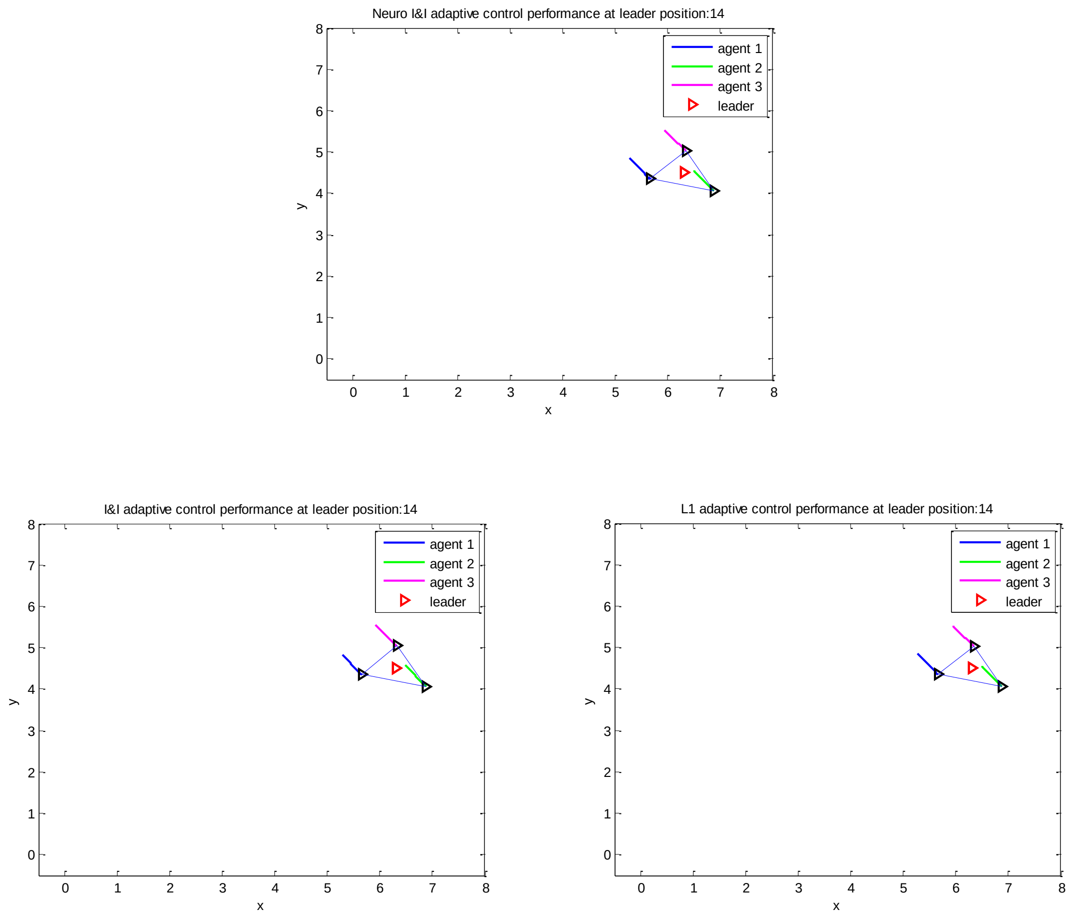

Figure 5.32 The group formation when the leader is at position $(\mathbf{6.3}, \mathbf{4.5})$.

Figure 5.32 shows the each agent move from position 6 to follow the leader at (6.3, 4.5). We can see the ability of neuro I&I, I&I and L1 adaptive controllers to navigate each agent to track the desired formation.

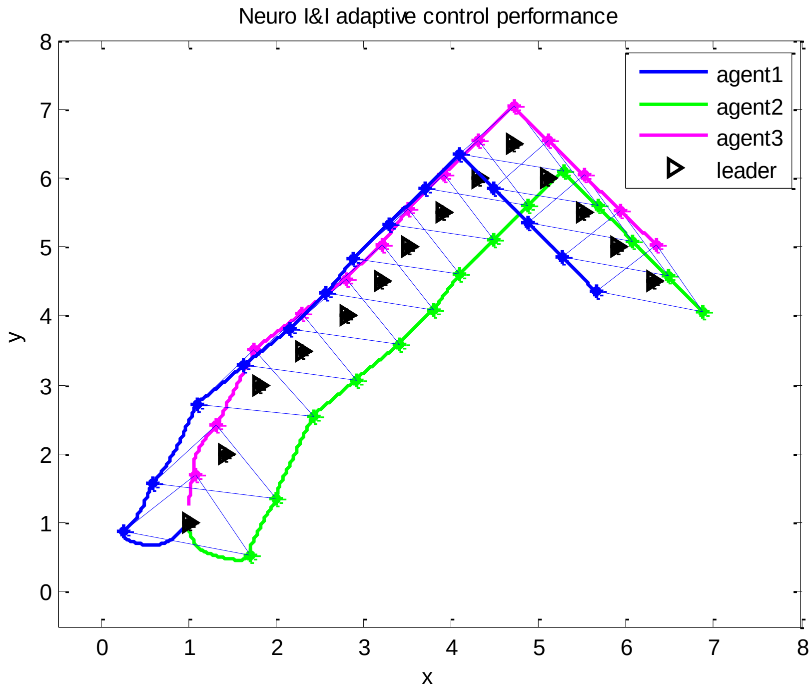

Figure 5.33 The group formation based neuro I&I adaptive control on unknown maps.

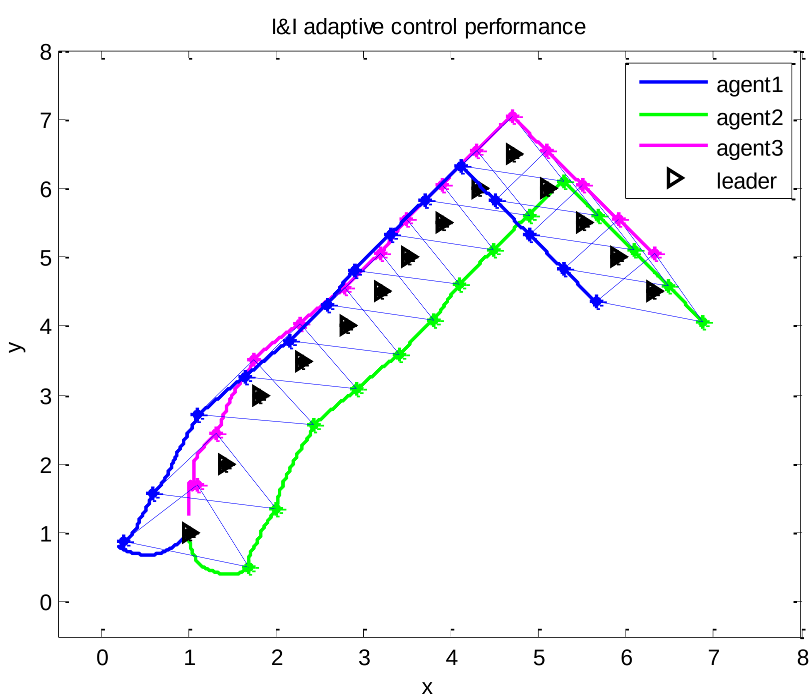

Figure 5.34 The group formation based I&I adaptive control on unknown maps.

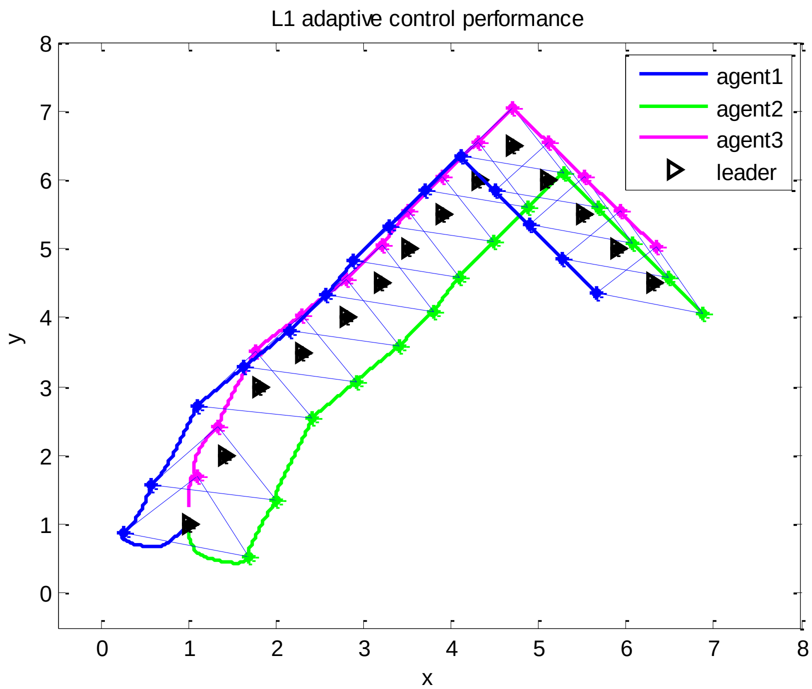

Figure 5.35 The group formation based L1 adaptive control on unknown maps.

Figure (5.33-5.35) show the comparison between neuro I&I, I&I and L1 adaptive controllers performance along the whole navigation trajectory. We can see the neuro I&I, I&I and L1 adaptive controllers are able to navigate each agent to track the desired formation. Table 5.2 shows the error position of formation control of nonholonomic mobile robots in percentage (%).

Table 5.3. Error position of formation control of nonholonomic mobile robots.\

No	Leader Position	Neuro I&I		I&I		L1	
		EL (%)	ER (%)	EL (%)	ER (%)	EL (%)	ER (%)
1	1	11.7659	11.4912	11.1852	10.965	11.3839	11.1243
2	2	14.6722	13.7286	14.4409	13.3639	14.463	13.4835
3	3	21.3977	21.5028	21.132	21.1455	21.4241	21.495
4	4	23.5163	23.6293	23.2554	23.311	23.3267	23.4135
5	5	24.9331	25.0157	24.6793	24.7219	24.7562	24.8199
6	6	26.0483	26.1022	25.8072	25.83	25.8836	25.9227
7	7	26.9495	26.9813	26.7243	26.7302	26.7971	26.8166
8	8	27.5632	27.5819	27.3464	27.3429	27.4182	27.4261
9	9	28.0435	28.0531	27.8366	27.8263	27.9072	27.907
10	10	28.4304	28.4335	28.2324	28.2171	28.3018	28.2958
11	11	28.035	28.0465	27.8323	27.8255	27.9026	27.9045
12	12	27.5429	27.5689	27.3359	27.3412	27.407	27.4222
13	13	26.9164	26.9637	26.7037	26.7272	26.7757	26.8107
14	14	26.0918	26.1725	25.8715	25.924	25.945	26.011

CHAPTER 6

CONCLUSION AND FUTURE WORK

6.1 Conclusions

In this thesis, a framework for cooperative control of heterogeneous systems based on I&I adaptive is developed. We compare the I&I adaptive with L1 adaptive control for formation control of heterogeneous robot that can be summarized as follows

1. I&I adaptive control demonstrate better performance than L1 adaptive control to track the desired formation on unknown trajectory.
2. Potential field based formation of heterogeneous systems is able to keep the distance of each agent and the center of robot moving together in particular formation.

We also compare the effectiveness of neuro I&I with I&I and L1 adaptive control for formation control of nonholonomic mobile robots that can be summarized as follows

1. All of the controllers, I&I, L1 and I&I adaptive control are able to track the desired formation on unknown trajectory.
2. Potential field based formation of nonholonomic mobile robots is able to keep the distance of each agent and the center of robot moving together in particular formation.

6.2 Future Work

1. The cooperative control on unknown map with obstacle avoidance will be good contribution.
2. One could look to implementation challenges and experimental validation of the control scheme proposed here.
3. Effect of communication and time delays could be investigated.

REFERENCES

[1] Fierro, R., and F. L. Lewis, "Control of nonholonomic mobile robot: backstepping kinematics into dynamics," Journal of Robotic Systems 14, no. 3, pp. 149–164, 1997.

[2] T. Fukao, H. Nakagawa, and N. Adachi, "Adaptive tracking control of a nonholonomic mobile robot," IEEE Transaction Robotics and Automation., vol. 16, no. 5, pp. 609–615, October 2000.

[3] Z. Cao, Y. Zhao, and Q. Wu, "Adaptive trajectory tracking control for a nonholonomic mobile robot," Chinese Journal of Mechanical Engineering, 24(3):1–7, 2011.

[4] D. H. Kim, J.-H. Oh, "Tracking control of a two-wheeled mobile robot using input–output linearization," Control Engineering Practice, 7 (3), pp. 369–373, 1999.

[5] J. Ye, "Tracking control of two-wheel driven mobile robot using compound sine function neural networks," Connection Science Volume 25, Issue 2-3, 2013.

[6] Imen, M., Mansouri, M. and Shoorehdeli, M.A., "Tracking control of mobile robot using ANFIS," Proceedings of the 2011 IEEE International Conference on Mechatronics and Automation, August 2011.

[7] O. Mohareri, R. Dhaouadi, A. B. Rad, "Indirect adaptive tracking control of a nonholomic mobile robot via neural networks," Neurocomputing, 88(1): 54-66, 2012.

[8] J. Huang, C. Wena, W. Wang, Z. P. Jiang, "Adaptive output feedback tracking control of a nonholonomic mobile robot," Automatica, Volume 50, Issue 3, Pages 821–831. March 2014.

[9] R. Fierro and F. L. Lewis, "Control of a nonholonomic mobile robot using neural networks," IEEE Transactions on Neural Networks, vol. 9, no. 4, pp.589 -600, 1998.

[10] A. Freddi, A. Lanzon, and S. Longhi, "A feedback linearization approach to fault tolerance in quadrotor vehicles," in Proceedings of The 2011 IFAC World Congress, Milan, Italy, 2011.

[11] D. Chwa, "Sliding-mode tracking control of nonholonomic wheeled mobile robots in polar coordinates," IEEE Transactions on Control Systems Technology, vol. 12, no. 4, pp.637 -644, 2004.

[12] T. Das and I. N. Kar, "Design and implementation of an adaptive fuzzy logic based controller of wheeled mobile robots," IEEE Transactions on Control Systems Technology, vol. 14, no. 3, pp.501 -510, 2006.

[13] T. Das , I. N. Kar and S. Chaudhury, "Simple neuron-based adaptive controller for a nonholonomic mobile robot including actuator dynamics," Neurocomputing, vol. 69, pp.2140 -2151, 2006.

[14] Jun Ye, "Adaptive control of nonlinear PID-based analog neural networks for a nonholonomic mobile robot," Neurocomputing, vol.71, pp.1561-1565, 2008.

[15] D. Chwa, "Tracking control of differential-drive wheeled mobile robots using a backstepping-like feedback linearization," IEEE Transaction on Systems, Man, and Cybernetics. A, vol. 40, no. 6, pp.1285 -1295, 2010.

[16] Z.P. Yuan, Z.P. Wang, and Q.J. Chen,"Trajectory tracking control of a nonholonomic mobile robot," 8th IEEE International Conference on Control and Automation, June, 2010.

[17] K. Shojaei, A. M. Shahri, and A. Tarakameh, "Adaptive feedback linearizing control of nonholonomic wheeled mobile robots in presence of parametric and nonparametric uncertainties," Robot. Computer-Integrated Manufacturing, 27, (1), pp. 194– 204, 2011.

[18] K. Shojaei and A. M. Shahri. "Output feedback tracking control of uncertain nonholonomic wheeled mobile robots: a dynamic surface control approach," IET Control Theory Applications, 6(2):n216-228, 2011.

[19] D. B. Lee, T. C. Burg, B. Xian, and D. M. Dawson, "Output feedback tracking control of an underactuated quad-rotor UAV," Proceedings of the American Control Conference, New York, pp. 1775-1780, July, 2007.

[20] Zhou Fang, Zhang Zhi, Liang Jun, and Wang Jian. "Feedback Linearization and Continuous Sliding Mode Control for a Quadrotor UAV," Proceedings of the 27th Chinese Control Conference. Kunming, China, pp. 349-353, 2008.

[21] T. Dierks, S. Jagannathan, "Neural network output feedback control of a quadrotor UAV," Proceeding of the IEEE Conference on Decision and Control, pp. 3633-3639, December 2008.

[22] D. Lee, H. J. Kim, and S. Sastry, "Feedback linearization vs. adaptive sliding mode control for a quadrotor helicopter," International Journal Control, Automation and Systems, 7(3), pp. 419-428, 2009.

[23] T. Lee, M. Leok, and N. McClamroch, "Geometric tracking control of a quadrotor UAV on SE(3)," Proceeding of the IEEE Conference on Decision and Control, pp. 5420-5425, 2010.

[24] C. Diao, B. Xian, Q. Yin, W. Zeng, H. Li, and Y. Yang, "A nonlinear adaptive control approach for quadrotor UAVs," 8th Asian Control Conference (ASCC), pp. 223-228, May 2011.

[25] Z. T. Dydek, A. M. Annaswamy, and E. Lavretsky, "Adaptive Control of Quadrotor UAVs: A Design Trade Study With Flight Evaluations," IEEE Transactions on Control Systems Technology, vol. 21, pp. 1400-1406, 2013.

[26] D. J. Lee, C. Ha and Z. Zuo, "Backstepping control of quadrotor-type UAVs: Trajectory tracking and teleoperation over the internet," Intelligent Autonomous Systems, pp. 217 -225, 2013.

[27] J. P. Desai, J. P. Ostrowski, and V. Kumar, "Controlling formations of multiple mobile robots," Proceedings 1998 IEEE Intemational Conference on Robotics & Automation, vol. 4, pp.2864 -2869, 1998.

[28] R. Fierro, A. Das, V. Kumar, and J. P. Ostrowski, "Hybrid control of formation of robots," Proceedings of the 2002 IEEE International Conference on Robotics 8 Automation, pp.157 -162, 2001.

[29] P. Song and V. Kumar, "A potential field based approach to multirobot manipulation," Proceedings of IEEE International Conference Robotics and Automation, pp.1217 -1222, 2002.

[30] L. Chaimowicz, N. Michael and V. Kumar. "Controlling Swarms of Robots Using Interpolated Implicit Functions," Proceedings of the IEEE International Conference on Robotics and Automation, pp. 2487-2492, April 2005.

[31] M. A. Hsieh and V. Kumar, "Pattern generation with multiple robots," Proceedings of the IEEE International Conference on Robotics and Automation, pp.2442 -2447, 2006

[32] T. Dierks and S. Jagannathan "Control of nonholonomic mobile robot formations: Backstepping kinematics into dynamics," 16th IEEE International Conference on Control Applications, pp.94 -99, 2007

[33] L. Sabattini, C. Secchi, and C. Fantuzzi, "Arbitrarily shaped formations of mobile robots: artificial potential fields and coordinate transformation," Autonomous Robots (Springer), vol. 30, pp. 385-397, 2011.

[34] J. Á. Acosta, R. Ortega, A. Astolfi, and I. Sarras. "A constructive solution for stabilization via immersion and invariance: The cart and pendulum system," Automatica, 44(9): pp. 2352–2357, 2008.

[35] T. WimboÌ´Lck, C. Ott, and G. Hirzinger. "Immersion and invariance control for an antagonistic joint with nonlinear mechanical stiffness," 49th IEEE Conference on Decision and Control, pages 1128–1135, 2010.

[36] N. S. Manjarekar, R. N. Banavar, and R. Ortega. "Stabilization of a synchronous generator with a controllable series capacitor via immersion and invariance," International Journal of Robust and Nonlinear Control, 2011.

[37] A. Astolfi, D. Karagiannis, and R. Ortega. "Nonlinear and adaptive control with applications," Springer Verlag, 2007.

[38] H. Goldstein. "Classical mechanics," Addison-Wesley, Reading, Ma, 1980.

[39] J. T. Wen. "Control of nonholonomic systems," The Control Handbook, pp 1359–1368, 1996.

[40] O. Alburaiki. "Leader-follower slam based navigation and fleet management control," Master Thesis at King Fahd University of Petroleum and Minerals, 2012.

[41] A. B. Koesdwiady, "Immersion and invariance control design for unmanned aerial vehicle," Master Thesis at King Fahd University of Petroleum and Minerals, 2013.

[42] N. Hovakimyan and C. Chengyu. "L1 adaptive control theory: guaranteed robustness with fast adaptation," Vol. 21. Siam, 2010.

[43] S. M. E. Elnaiem, "Adaptive formation control of a fleet of underwater vehicle-manipulator system," Master Thesis at King Fahd University of Petroleum and Minerals, 2014.

Vita

Name : Imil Hamda Imran

Nationality : Indonesia

Date of Birth : 2/28/1988

Email : g201206020@kfupm.edu.sa, imilhamda62@gmail.com

Address : Balai Panjang Payakumbuh, Indonesia

Academic Background : MS in Systems Engineering (Major: Systems and Control)
KFUPM, Dhahran 2015
BS in Electronics and Communications Engineering,
Andalas University 2011

Publications:

1. Sami El Ferik, Imil Hamda Imran. “Control of Nonholonomic Mobile Robot Based on Immersion and Invariance Adaptive Control”. 12th International Multi-Conference on Systems, Signals and Devices, 2015.
2. Sami El Ferik, Tri Bagus Susilo, Muhammad Fahrudin Muna, Imil Hamda Imran. “Stiction Compensation Using PI-Sliding Mode Control for Pneumatic Valve”. 12th International Multi-Conference on Systems, Signals and Devices. 12th International Multi-Conference on Systems, Signals and Devices, 2015.